

# POLITECNICO DI TORINO

Engineering Faculty

## MASTER THESIS IN MECHATRONIC ENGINEERING

*Modeling and experimental validation of a complete system of a wheel loader for oscillations reduction in ride conditions*



**Advisors:**

Prof. Luigi Mazza

Prof. Andrea Vacca

**Candidate:**

Riccardo Madau

ACADEMIC YEAR 2017-2018



*To my family, my friends and all the people that supported me in this  
long and challenging journey.*



# Contents

<b>1</b>	<b>Introduction</b>	<b>6</b>
1.1	Problem overview . . . . .	6
1.2	Reference machine . . . . .	7
1.3	Aim of the Thesis . . . . .	8
1.4	Outline of the Thesis . . . . .	9
<b>2</b>	<b>State of the art</b>	<b>10</b>
2.1	Hydro-Mechanical method . . . . .	10
2.2	Electro-Hydraulic method . . . . .	12
2.2.1	Valveless pump displacement control . . . . .	12
2.2.2	Proportional directional valve control . . . . .	13
2.3	Discussion of the suggested project method . . . . .	14
<b>3</b>	<b>Vehicle analytical model</b>	<b>15</b>
3.1	Vehicle dynamics . . . . .	15
3.1.1	Chassis model . . . . .	18
3.1.2	Boom model . . . . .	19
3.1.3	Wheels model . . . . .	20
3.1.4	Boom actuator geometry . . . . .	24
3.1.5	Kinematic constraint . . . . .	26
3.1.6	Equations derivation . . . . .	28
3.2	Hydraulics . . . . .	31
3.2.1	Hydraulic actuator . . . . .	32
3.2.2	Supply dynamics . . . . .	34
3.3	Complete model . . . . .	37
3.4	Model validation . . . . .	38
3.4.1	Case 1 . . . . .	39
3.4.2	Case 2 . . . . .	40
<b>4</b>	<b>Control strategy</b>	<b>41</b>
4.1	Control structure . . . . .	41

4.2	Feedback choice . . . . .	42
4.3	Controller design . . . . .	44
	4.3.1 Plant model deduction . . . . .	44
	4.3.2 Filter implementation . . . . .	47
4.4	Simulation results . . . . .	58
	4.4.1 Case 1 . . . . .	58
	4.4.2 Case 2 . . . . .	59
<b>5</b>	<b>Experimental results</b>	<b>60</b>
5.1	From model to real vehicle . . . . .	60
5.2	Position control . . . . .	62
5.3	Complete controller . . . . .	65
	5.3.1 Case 1 . . . . .	65
	5.3.2 Case 2 . . . . .	67
<b>6</b>	<b>Conclusions</b>	<b>68</b>
<b>7</b>	<b>Future work</b>	<b>71</b>

# List of Figures

- 1.1 Uneven road oscillation transmission . . . . . 6
- 1.2 Reference Machine, *Wheel Loader* CASE 721f . . . . . 7
- 2.1 Example of common current implementation, *Passive Ride Control* (PRC) . . . . . 11
- 2.2 Variable Displacement Valveless Control . . . . . 12
- 2.3 Proportional Directional Valve Control . . . . . 13
- 3.1 Reference Machine Kinematics . . . . . 16
- 3.2 Vector of the radius between two points . . . . . 17
- 3.3 Chassis force balance equations . . . . . 18
- 3.4 Boom force balance equations . . . . . 19
- 3.5 Wheels spring-damping modeling . . . . . 21
- 3.6 Road profile example . . . . . 23
- 3.7 Hydraulic boom actuator geometry . . . . . 24
- 3.8 Implement geometry and piston position . . . . . 25
- 3.9 Kinematic constraint . . . . . 27
- 3.10 Asymmetric linear actuator . . . . . 32
- 3.11 Simplified hydraulic schematic . . . . . 34
- 3.12 Simplified schematic of directional valve and implement . . . . . 35
- 3.13 Schematic of the model structure . . . . . 37
- 3.14 First test case validation results . . . . . 39
- 3.15 Second test case validation results . . . . . 40
- 4.1 Schematic of the acceleration feedback control structure . . . . . 43
- 4.2 Applied schematic of the pressure feedback control logic . . . . . 43
- 4.3 Schematic of the pressure feedback control structure . . . . . 46
- 4.4 Simplified schematic of the control structure . . . . . 47
- 4.5 Simulation results for test without control . . . . . 48
- 4.6 Structure modification for root locus method . . . . . 49
- 4.7 Root locus plot with LP filter, when  $\tau$  is constant on each curve and  $K_f$  varies . . . . . 51

4.8	Comparison of simulation results with LP filter applied and not . . . . .	52
4.9	Root locus plot with HP filter, when $\tau$ is constant on each curve and $K_f$ varies . . . . .	53
4.10	Comparison of simulation results with HP filter applied and not . . . . .	54
4.11	Comparison of simulation results with respect to uncompensated system . . . . .	55
4.12	Filtered signals delay . . . . .	57
4.13	First test case control simulation results . . . . .	58
4.14	Second test case control simulation results . . . . .	59
5.1	First test case control experimental results . . . . .	61
5.2	Structure schematic with the additional boom angle control loop . . . . .	62
5.3	State flow for the PD control logic . . . . .	63
5.4	PD logic applied, positive input command only . . . . .	64
5.5	Case 1: experimental results long period T . . . . .	65
5.6	Case 1: experimental results short period T . . . . .	66
5.7	Case 2: experimental results short period T . . . . .	67
6.1	Comparison between no control, ARC and PRC . . . . .	69
6.2	Driveway test, vertical cabin acceleration . . . . .	69
6.3	Driveway test, boom angle . . . . .	70
7.1	First test case control results . . . . .	72
7.2	Second test case control results . . . . .	72

# Chapter 1

## Introduction

This introductory chapter will first describe the motivation of the research, briefly presenting an overview of the problem. The machine, on which the issue has been analyzed, will then be described. Afterwards, the objective and the structure of the thesis will be explained.

### 1.1 Problem overview

During typical work cycles, earthmoving machines are usually involved in handling heavy loads. Since high stiffness is necessary in order to carry weight, wheel suspensions are not commonly included. Because of this, in driving conditions, the vibrations introduced by the road are directly transmitted to the vehicle chassis and arm.



Figure 1.1: Uneven road oscillation transmission

Due to the introduced vibrations, the machine is negatively affected. The stability of the load could be influenced, causing the material to fall from the bucket and the consequent working efficiency reduction. Moreover, since the transmitted oscillations have usually a strong low frequency component, machine handling and stability, besides driver comfort, are compromised. All these effects decrease vehicle safety, productivity and life span.

## 1.2 Reference machine

One of the off-road vehicles mostly affected by this problem is the Wheel Loader. For this reason, the chosen reference machine is a loader CASE 721f model. Around 15000 kg of operating weight, composed by a rear part, called tractor, and a front loader, front axle and arm. Between the two parts, a pivot point allows the hydraulically actuated steering system to maneuver the machine.

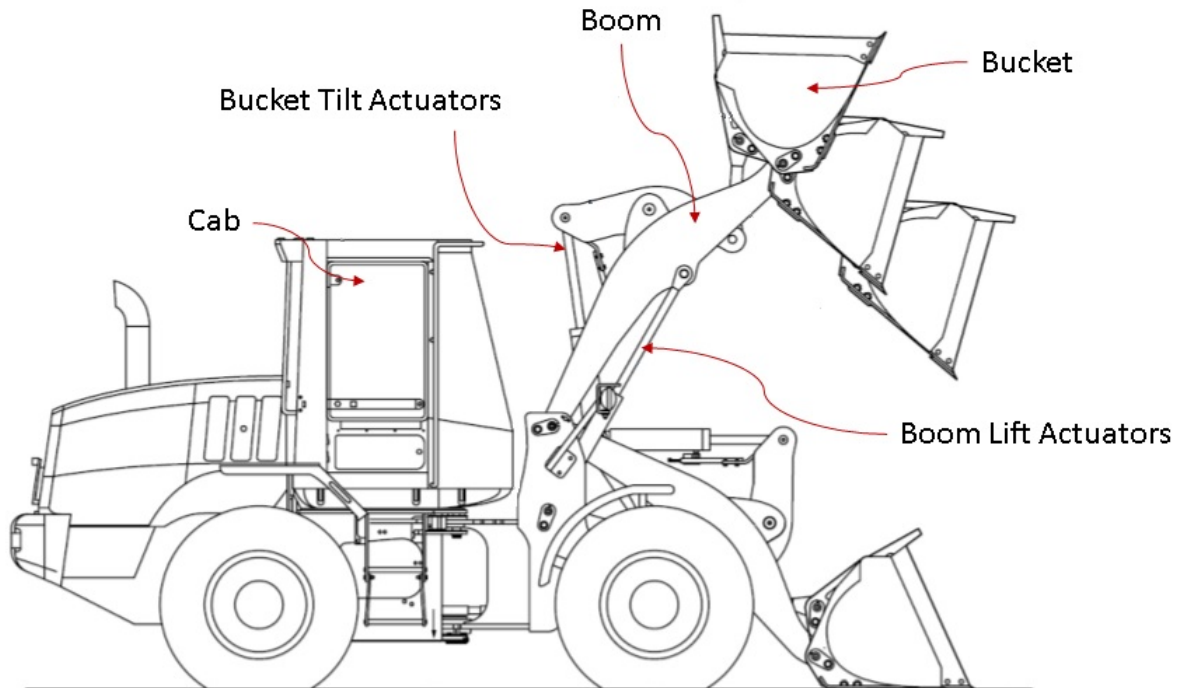


Figure 1.2: Reference Machine, *Wheel Loader CASE 721f*

The propulsion is provided by a diesel engine, which is also used for driving the pumps on the hydraulic circuitry. The boom is actuated by two lift hydraulic actuators, for raising and lowering movements. A tilt cylinder is also mounted, to change the orientation of the bucket, for performing loading and dumping cycles.

### 1.3 Aim of the Thesis

Since the wheel loader is capable of carrying heavy loads in the bucket, it is exploitable for transporting loaded material. Because of the uneven road, on which this vehicle usually is driven, and due to the lack of wheel suspensions, different solutions have been proposed in the past. The most diffused method is the so called "*Passive Ride Control*" (PRC). These systems often integrate additional hydraulic elements in the circuitry. Even if the passive solution can produce a good improvement, it's expensive and, being optimized for a single operating condition, is not always properly effective.

Those limitations lead to the investigation of alternative solutions. In fact, an *active* strategy, not currently available in commercial machines, could overcome the constraints of the passive method. Using the standard hydraulic architecture, it could realize the same counter-acting action, sending an electronic signal to command the boom actuators movement, in order to compensate the oscillations induced by the ground. The "*Active Ride Control*" (ARC) allows to save on additional expensive components and has a potentially infinite range of working effectiveness.

Indeed, the aim of the project is to develop an ARC, suitable for the reference vehicle, able to reduce the cabin oscillations, thus providing:

- productivity improvement;
- better handling, stability and safety;
- better comfort for the driver.

## 1.4 Outline of the Thesis

A more exhaustive description of the past solutions will be presented through the State of the Art. Then, a mathematical model of the vehicle will be showed and compared with respect to the acquired experimental data. After that, an explanation on how the control structure has been chosen will be described. The results of the applied control strategy will be analyzed and, eventually, the main points of the thesis summarized in the conclusions.

Besides, a possibility of further work is suggested in the last chapter.

# Chapter 2

## State of the art

This chapter presents different ride control methods for the wheel loader case. The categories are distinguished according to the used technology : hydro-mechanical and electro-hydraulic methods. Benefits and drawbacks of the strategies will be pointed out.

### 2.1 Hydro-Mechanical method

As the name suggests, the Hydro-Mechanical method only involves hydraulic and mechanical fields. This means that all the modifications applied to the system belong to these two domains.

The additional components, typically used in order to reduce the oscillations in driving conditions, are the following:

1. hydraulic resistance;
2. hydraulic capacitance.

The resistance is used to dissipate the vibration energy and it is usually obtained by including an orifice in the hydraulic circuit.

An hydraulic accumulator, instead, is typically added to perform the capacitance function: modify the system responsiveness. The Passive Ride Control (PRC), previously introduced, takes advantage of the combination of the two elements to improve the system behavior. With this method, currently commercialized, the additional components are placed close to the boom actuators ports, interfacing with the directional control valve, that manages the flow to and from the cylinders.

An implementation example of the PRC is showed in Figure 2.1. The solenoid actuated valve (3), if excited, switches the position of the *Ride Control Spool Valve* (2), that allows the fluid, present in the lift cylinders, to enter the *Ride Control Valve* (1). The oscillations of the pistons produce a flow going back and forth between the cylinders and the additional accumulator (6). The hydraulic capacitance is able to slow down this dynamics, while the resistance of the spool valve dissipates the oscillation energy of the fluid. The *Pressure Relief Valve* (4) is active when the pressure in the line is higher than the established one, while the *Manual Bleed Valve* (5) is used in case the accumulator has to be emptied, sending the flow to tank.

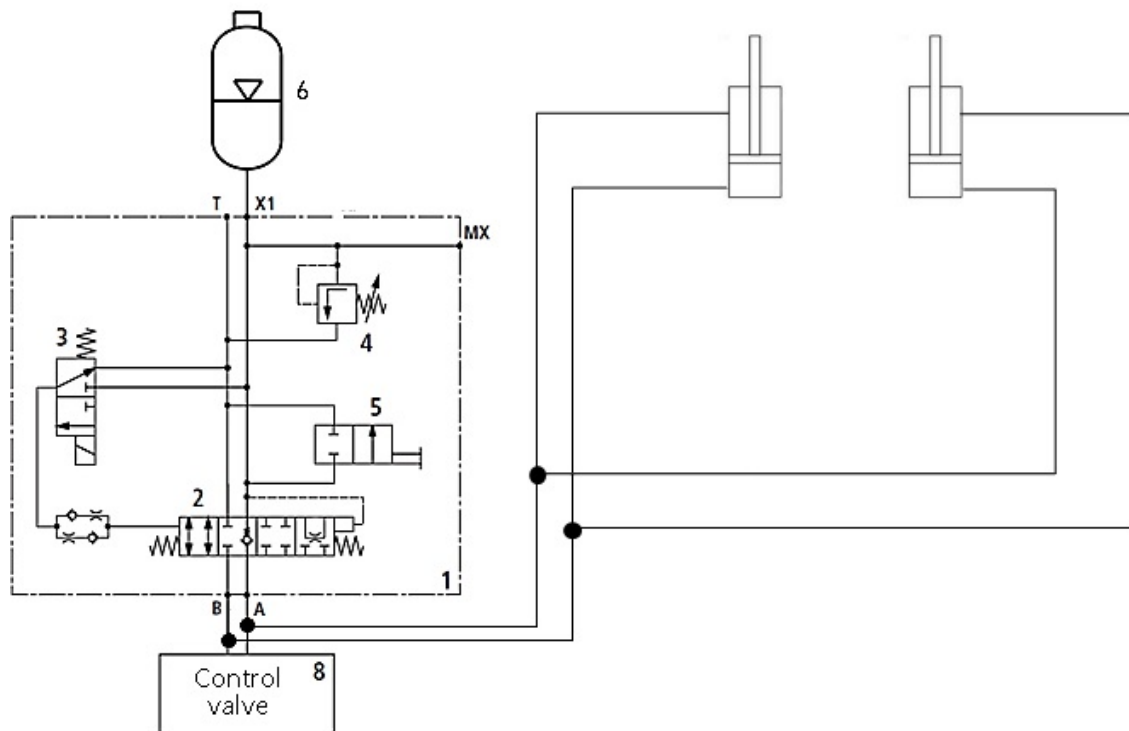


Figure 2.1: Example of common current implementation, *Passive Ride Control* (PRC)

Being the PRC an hydro-mechanical method, the parameters, that have to be chosen to size the components, are fixed. Therefore, the more the conditions are different from the nominal ones, the more the improvement is limited. A pressure feedback signal have been introduced to allow a wider range of proper effectiveness. Anyway, with respect to the standard circuit, the use of the PRC increases cost, complexity, volume and weight.

## 2.2 Electro-Hydraulic method

The Active Ride Control is included in the electro-hydraulic methods. Differently from the passive technique, since the boom actuators are "actively" controlled, in order to work, this solution requires electric energy from the wheel loader power supply.

As previously highlighted in the Section 1.3 of the first chapter, the active solution does not need additional components to perform the requested task. Beside that, every electronic signal, coming from the sensors, can be acquired and utilized as feedback signal. The control strategy becomes *adaptive* by switching logic and parameters, ensuring optimal control in different working conditions. Additionally, it potentially increases the energy management efficiency and reduces the overall costs.

Over the past years, two different application of the concept have been studied for the wheel loader case :

- valveless pump displacement control
- proportional directional valve control

### 2.2.1 Valveless pump displacement control

The basic concept of the variable displacement control, without proportional directional valve, is to directly manage the hydraulic actuators, saving space and components.

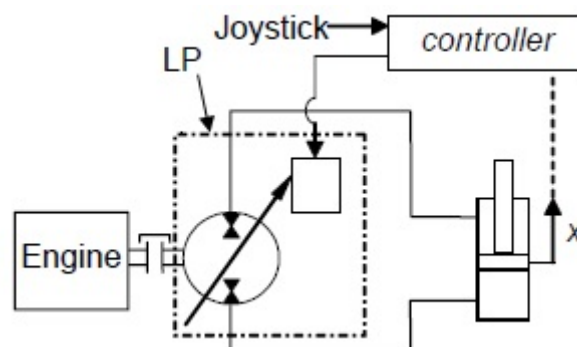


Figure 2.2: Variable Displacement Valveless Control

In Figure 2.2 the controller vary the pump displacement depending on the received user joystick command and piston position signals. The actuator is then driven by the flow coming from the pump. A Low Pressure (LP) level is utilized to supply the pump control system.

### 2.2.2 Proportional directional valve control

In this project, the reference wheel loader was provided of a directional valve for the boom actuation.

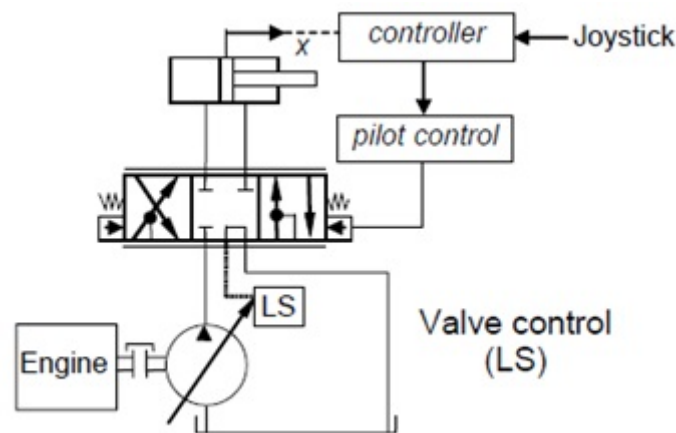


Figure 2.3: Proportional Directional Valve Control

As in Figure 2.3 the typical system is supplied by a Load Sensing (LS) pump. The controller works as in the displacement control system, but, instead of acting on the displacement of the pump, it energizes the electric pilot stages of the valve (usually composed by solenoids). By modifying the spool position of the directional valve, and consequently varying the load impact, it is possible to indirectly control the pump.

## 2.3 Discussion of the suggested project method

In the recent past, different control techniques have been studied for building an ARC method to be implemented on wheel loaders, equipped with proportional directional valves. Model-based and frequency-based methods, with different compositions of feedback signals, have been examined trying to find the best procedure for the oscillation reduction. In both cases the improvements in the simulation results were perceptible, but the experimental outcomes, due to real-time implementation difficulties, were not as satisfying.

For this reason, I started studying the problem, having the target of simplifying the control structure, in order to make the strategy as much effective as possible.

# Chapter 3

## Vehicle analytical model

In order to understand the behavior of the vehicle, when subject to the strain the road is capable of inducing on it, and for achieving appreciable control results, a simulation model has to be obtained. In this Chapter an explanation on how an analytical model has been derived will be presented. A dynamic analysis of the vehicle, coupled with the dynamic of the wheels is modeled. Besides, a simple model of the hydraulic circuitry actuating the boom will be showed. The effect of the bucket movement on the oscillation reduction, during driving conditions, is assumed to be irrelevant. For this reason and since the bucket is not supposed to be tilted, for ensuring stability to the loaded material, the tilt actuators are not modeled.

### 3.1 Vehicle dynamics

The dynamics of the vehicle is based on force balance equations applied to the highlighted points on Figure 3.1, in which the equations are modeled for horizontal, vertical and moment equation. The machine is analyzed on a two-degree of freedom base because vertical and horizontal are the mostly stressed directions. The impact of third component is neglected because not relevant with respect to the others.

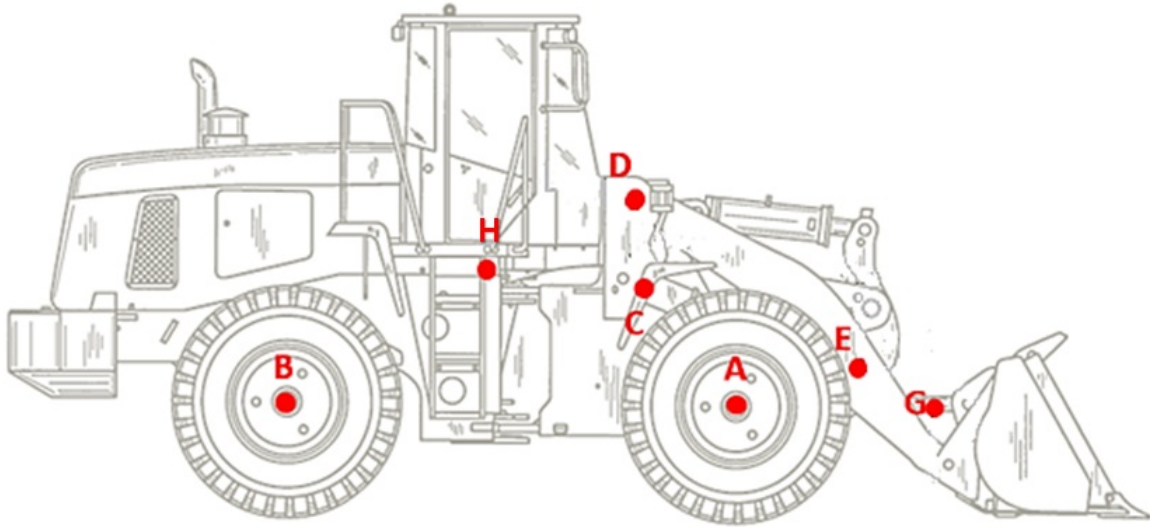


Figure 3.1: Reference Machine Kinematics

These points have been considered because of their relevance:

- A,B center of front and rear wheels
- H center of gravity of the tractor
- D center of rotation of the arm
- G center of gravity of the arm
- C,E points of contact between actuators and the rest of the system

When the control is active, the arm is moving. Then, tractor and implement move relative to each other. For this reason the vehicle is first decoupled into tractor, or chassis, and boom, or implement. The two parts of the machine are connected by the points C and D. Since the two parts are treated as distinguished rigid bodies, each fraction is characterized by its own force balance equations.

In the following expressions, the symbols  $m_1, J_1$  and  $m_2, J_2$  correspond to mass and rotational inertia of chassis (1) and implement (2). The variables  $F_{**}$ , instead, are forces whose first element is related to the highlighted point where it is applied, while the second one is the axis on which it is directed, with the versus indicated by the arrow in the figure.

For example:

$F_{By}$ , is the force applied in B whose direction is on the vertical axis. The components  $F_{D12y}$  and  $F_{D12x}$  are so called because applied in both chassis and boom. The constants  $m_1g$  and  $m_2g$  are the gravitational effect of the two masses of the bodies.

The indication of the distance between the points is made using the following nomenclature:

$r_{123}$ , where r stands for radius, 1 and 2 are the two points, while 3 is the axial component of the distance, for which the angle between the points is needed.

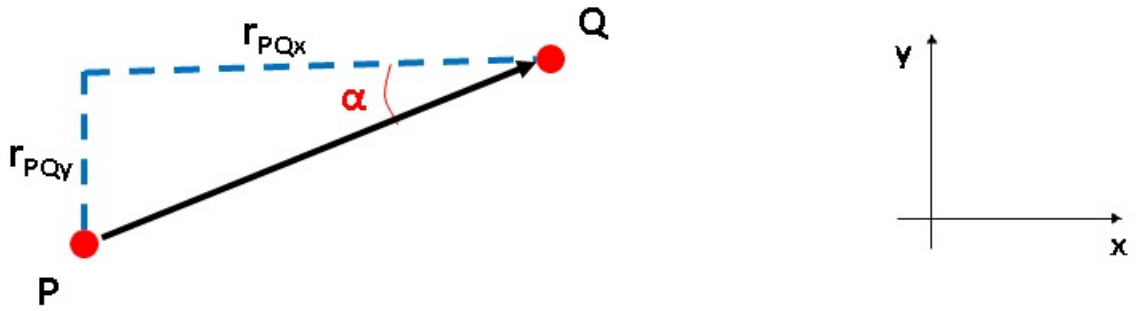


Figure 3.2: Vector of the radius between two points

In the following table 3.1, the parameters exploited with respect to the global fixed reference frame:

Parameter	Complete expression
$r_{AHx}$	$r_{AH}\cos(\vartheta_{AH} + \vartheta_1)$
$r_{AHy}$	$r_{AH}\sin(\vartheta_{AH} + \vartheta_1)$
$r_{BHx}$	$r_{BH}\cos(\vartheta_{BH} + \vartheta_1)$
$r_{BHy}$	$r_{BH}\sin(\vartheta_{BH} + \vartheta_1)$
$r_{CHx}$	$r_{CH}\cos(\vartheta_{CH} + \vartheta_1)$
$r_{CHy}$	$r_{CH}\sin(\vartheta_{CH} + \vartheta_1)$
$r_{DHx}$	$r_{DH}\cos(\vartheta_{DH} + \vartheta_1)$
$r_{DHy}$	$r_{DH}\sin(\vartheta_{DH} + \vartheta_1)$
$r_{DGx}$	$r_{DG}\cos(\vartheta_{DG} + \vartheta_2)$
$r_{Dgy}$	$r_{DG}\sin(\vartheta_{DG} + \vartheta_2)$
$r_{EGx}$	$r_{EG}\cos(\vartheta_{EG} + \vartheta_2)$
$r_{EGy}$	$r_{EG}\sin(\vartheta_{EG} + \vartheta_2)$

Table 3.1: Highlighted points distance variables

The terms involved in the application are composed by a constant part, distances and angles between the points, measured when the vehicle is steady and the boom angle is aligned with the global horizontal axis, and a variable component,  $\vartheta_1$  and  $\vartheta_2$ . So that, while the machine is moving, and there is a pitching action or the arm is actuated, the distance parameters change accordingly.

### 3.1.1 Chassis model

The followings are the starting equations related to the chassis:

$$m_1 \ddot{x}_H = F_{Ax} + F_{Bx} + F_{Cx} + F_{D12x} \quad (3.1)$$

$$m_1 \ddot{y}_H = F_{Ay} + F_{By} + F_{Cy} + F_{D12y} - m_1 g \quad (3.2)$$

$$J_1 \ddot{\vartheta}_1 = F_{Ay} r_{AHx} + F_{Ax} r_{AHy} - F_{By} r_{BHx} + F_{Bx} r_{BHy} + F_{Cy} r_{CHx} + F_{Cx} r_{CHy} + F_{D12y} r_{DHx} - F_{D12x} r_{DHy} \quad (3.3)$$

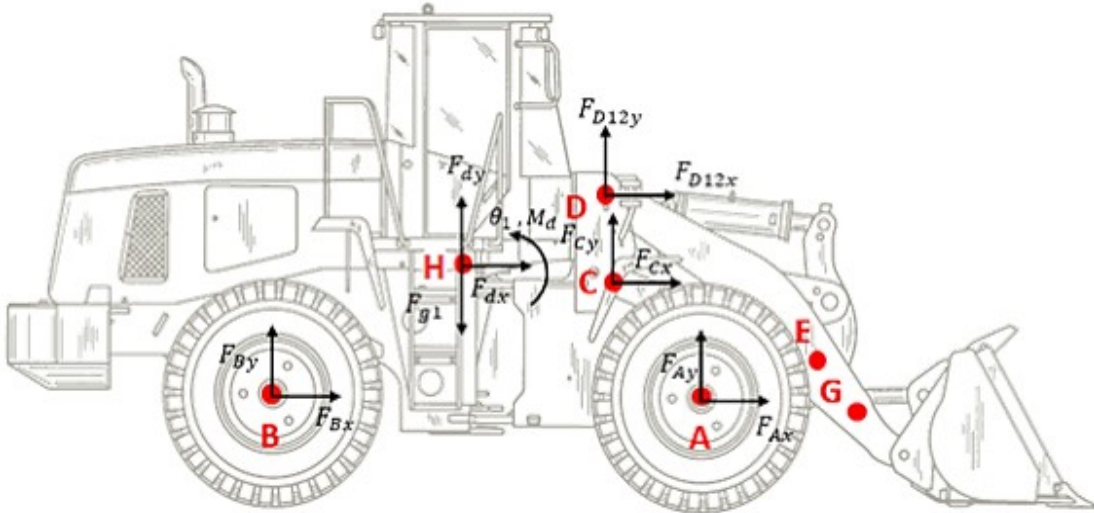


Figure 3.3: Chassis force balance equations

In the moment equation, the fixed axis is positioned in the tractor center of gravity H, and the positive sign is considered to be anticlockwise.  $\vartheta_1$  is the angle correspondent to the orientation of the tractor with respect to the horizontal axis. The positive direction for vertical and horizontal equations are upward and rightward, respectively.

### 3.1.2 Boom model

The followings are the starting equations related to the boom:

$$m_2\ddot{x}_G = -F_{D12x} + F_{Ex} \quad (3.4)$$

$$m_2\ddot{y}_G = -F_{D12y} + F_{Ey} - m_2g \quad (3.5)$$

$$J_2\ddot{\vartheta}_2 = -F_{Ey}r_{EGx} - F_{Ex}r_{EGy} + F_{D12x}r_{DGy} + F_{D12y}r_{DGx} \quad (3.6)$$

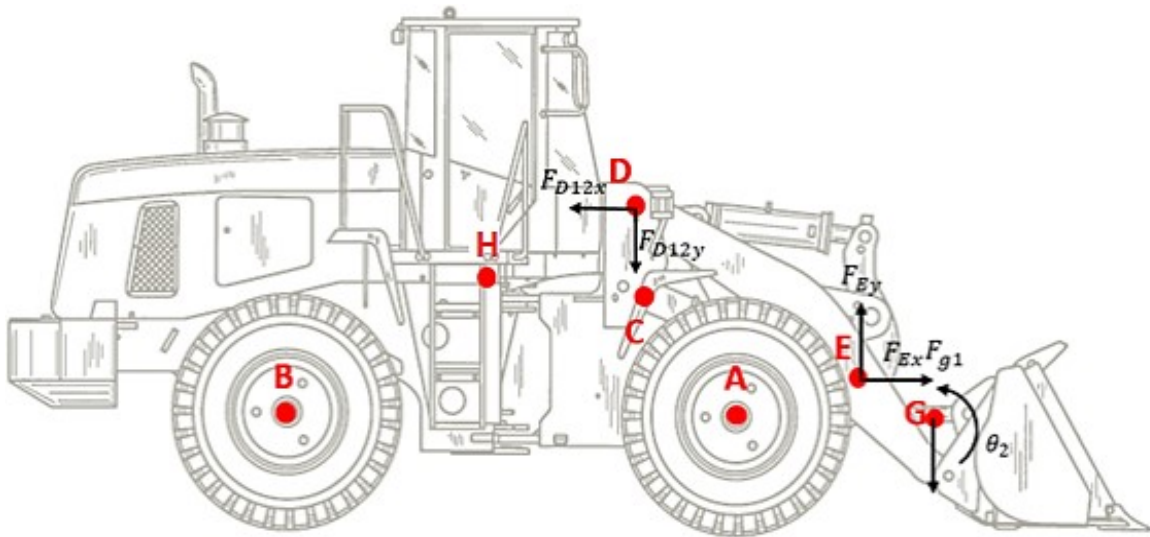


Figure 3.4: Boom force balance equations

In the moment equation, the fixed axis is positioned in the arm center of gravity G, and the positive sign is considered to be anticlockwise.  $\vartheta_2$  is the angle correspondent to the orientation of the segment DG with respect to the horizontal axis. The positive direction for vertical and horizontal equations are upward and rightward, respectively.

### 3.1.3 Wheels model

#### Wheels dynamics

For what concern the interaction between ground and vehicle, the wheels are modeled as a two-dimensional (2D) *spring-damping* system. The parameters  $c_{ty}$  and  $k_{ty}$  are the spring damping vertical rates for the tires. The same definition applies for the horizontal parameters  $c_{tx}$  and  $k_{tx}$ . Besides, these values can change in time, for example for variations of tire pressure or wear. Since they are of difficult derivation, they are obtained from experimental results and, for easiness, they are kept at a reasonable constant value.  $x_{AR}$  (or  $x_{BR}$ ) and  $y_{AR}$  (or  $y_{BR}$ ) correspond to the displacement of the disturbance input of the road profile, that affects the tires behavior, position and velocity, on the front (or rear) axle. An additional term is considered due to possible alterations of the pitching moment.

$$F_{Ax} = -k_{tx}\Delta x_A - c_{tx}\Delta \dot{x}_A \quad (3.7)$$

$$F_{Ay} = -k_{ty}\Delta y_A - c_{ty}\Delta \dot{y}_A \quad (3.8)$$

$$F_{Bx} = -k_{tx}\Delta x_B - c_{tx}\Delta \dot{x}_B \quad (3.9)$$

$$F_{By} = -k_{ty}\Delta y_B - c_{ty}\Delta \dot{y}_B \quad (3.10)$$

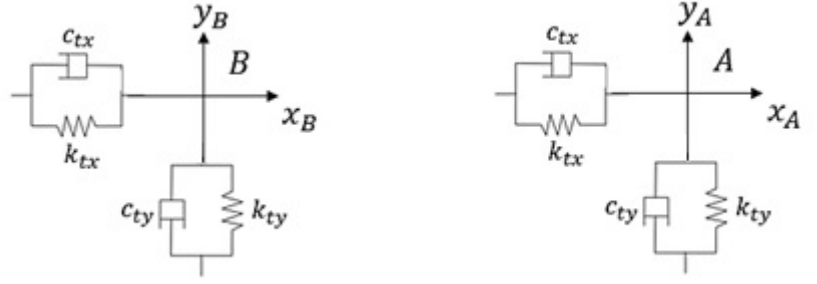


Figure 3.5: Wheels spring-damping modeling

The range of the wheels position variation corresponds to:

$$\Delta x_A = x_H - x_{AR} + \vartheta_1 r_{AHy} \quad (3.11)$$

$$\Delta y_A = y_H - y_{AR} + \vartheta_1 r_{AHx} \quad (3.12)$$

$$\Delta x_B = x_H - x_{BR} + \vartheta_1 r_{BHx} \quad (3.13)$$

$$\Delta y_B = y_H - y_{BR} - \vartheta_1 r_{BHy} \quad (3.14)$$

Whose derivatives are:

$$\Delta \dot{x}_A = \dot{x}_H - \dot{x}_{AR} + \dot{\vartheta}_1 r_{AHy} \quad (3.15)$$

$$\Delta \dot{y}_A = \dot{y}_H - \dot{y}_{AR} + \dot{\vartheta}_1 r_{AHx} \quad (3.16)$$

$$\Delta \dot{x}_B = \dot{x}_H - \dot{x}_{BR} + \dot{\vartheta}_1 r_{BHx} \quad (3.17)$$

$$\Delta \dot{y}_B = \dot{y}_H - \dot{y}_{BR} - \dot{\vartheta}_1 r_{BHy} \quad (3.18)$$

Now, the forces applied to the center of the wheels can be derived:

$$F_{Ax} = -k_{tx}(x_H - x_{AR} + \vartheta_1 r_{AHy}) - c_{tx}(\dot{x}_H - \dot{x}_{AR} + r_{AHy} \dot{\vartheta}_1) \quad (3.19)$$

$$F_{Ay} = -k_{ty}(y_H - y_{AR} + \vartheta_1 r_{AHx}) - c_{ty}(\dot{y}_H - \dot{y}_{AR} + r_{AHx} \dot{\vartheta}_1) \quad (3.20)$$

$$F_{Bx} = -k_{tx}(x_H - x_{BR} + \vartheta_1 r_{BHx}) - c_{tx}(\dot{x}_H - \dot{x}_{BR} + r_{BHx} \dot{\vartheta}_1) \quad (3.21)$$

$$F_{By} = -k_{ty}(y_H - y_{BR} + \vartheta_1 r_{BHy}) - c_{ty}(\dot{y}_H - \dot{y}_{BR} + r_{BHy} \dot{\vartheta}_1) \quad (3.22)$$

From the equations written above, it is evident that the forces applied to the center of the wheels are strongly dependent on the displacement of the road profile, plus a less relevant, but present, pitching component.

### Road disturbances

The road profile defines the wheel motion and thus, how the vehicle is stressed. An easy way to model it is to define its trajectory, combining a defined path with a certain amount of time necessary to complete the task.

Since the main oscillations on the cab come from vertical disturbances, the road profile has been defined only along the  $y$  axis. For this reason, the path is differently defined for front and rear wheels. This distinction is made so that, if the two axles meet distinct street displacements, the user can shape them accordingly.

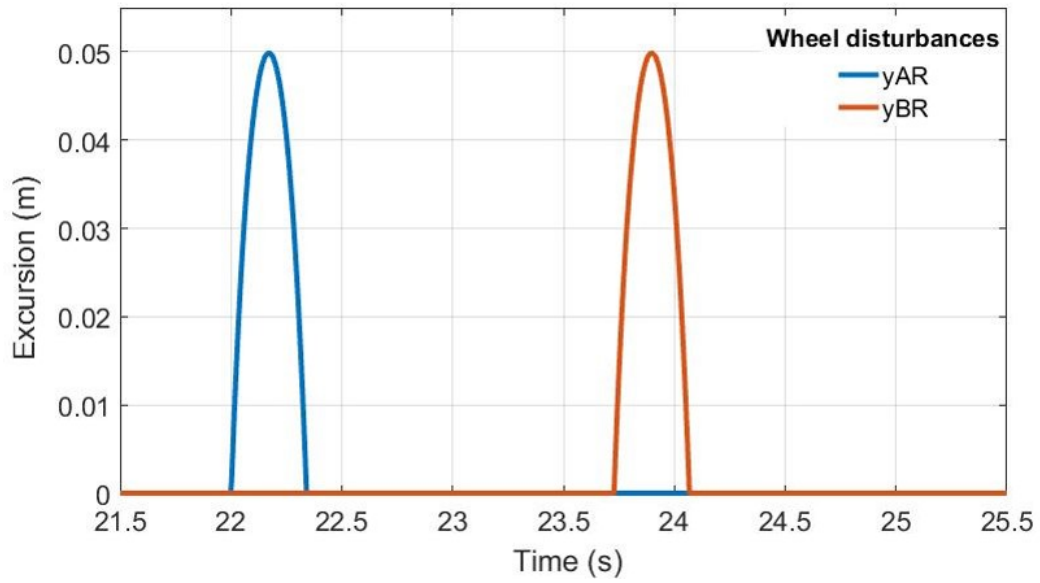


Figure 3.6: Road profile example

In the figure 3.6 above, it is presented an example of how the road is modeled: time variant path, with vertical excursion for each pair of wheels. In this case, the street profile is represented by a speed-bump, that will then be used as a model validation test.

### 3.1.4 Boom actuator geometry

Since the points C and E are the boom actuators ends, and assuming the fluid condition close to the incompressibility, it can be said that :

$$F_{Ex} = -F_{Cx} \quad (3.23)$$

$$F_{Ey} = -F_{Cy} \quad (3.24)$$

Besides, neglecting the effect of friction and loss components, insignificant with respect to the entity of the forces caused by the pressure inside the cylinders, they can also be translated into external force applied to the hydraulic actuator  $F_{cyl}$ . In Figure 3.7, C, D and E are the points belonging to the wheel loader and the cylinder shown is the one used for the motion of the arm.  $p_A$  and  $Q_A$  are pressure and flow rate related to the piston side of the body, while  $p_B$  and  $Q_B$  are the parameters on the rod side. The angle, between an imaginary line, parallel to the rod, and the horizontal axis of the chassis mobile reference frame, is called  $\gamma$ .

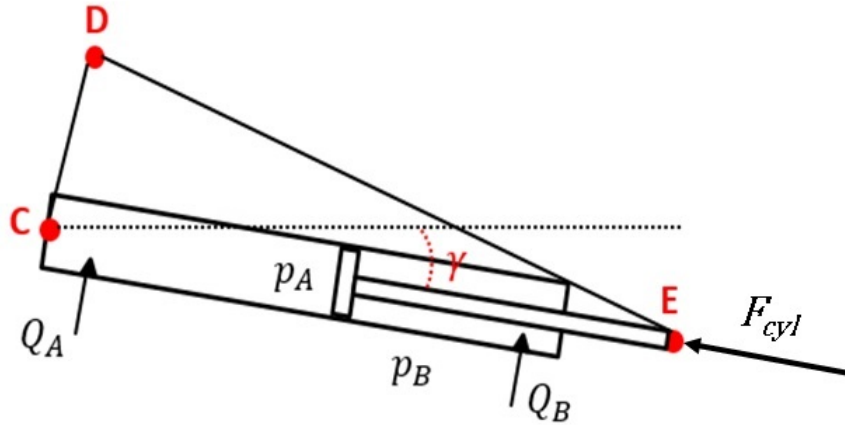


Figure 3.7: Hydraulic boom actuator geometry

$$F_{Ex} = F_{cyl} \cos(\gamma) \quad (3.25)$$

$$F_{Ey} = -F_{cyl} \sin(\gamma) \quad (3.26)$$

Besides, referring to figure 3.7, it can be also achieved a geometric relationship between  $\gamma$  and  $\vartheta_2$ :

$$\gamma = \text{atan}\left(\frac{r_{DEy} - r_{DCy}}{r_{DEx} + r_{DCx}}\right) \quad (3.27)$$

Another useful relation able to reduce the number of variables in the system, is to link  $\vartheta_2$  and the piston position  $x_{cyl}$  and velocity  $\dot{x}_{cyl}$ .

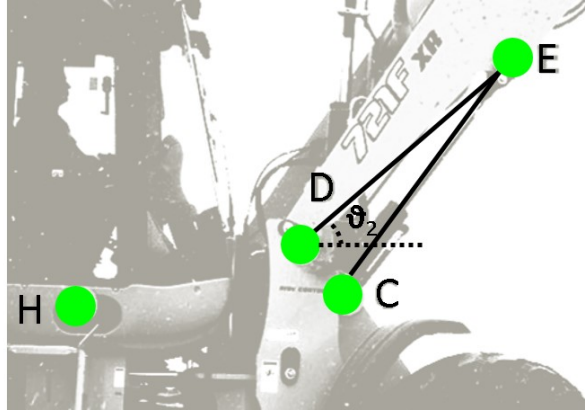


Figure 3.8: Implement geometry and piston position

Starting from the relationship between current length of the cylinder  $r_{CE}$  and piston position  $x_{cyl}$ :

$$x_{cyl} - x_{cyl}^0 = l_{cyl} - l_{cyl}^0 \quad (3.28)$$

Where  $x_{cyl}^0$  and  $l_{cyl}^0$  correspond to the length of cylinder and piston position, when the piston is completely retracted.

From which:

$$x_{cyl} = \sqrt{(r_{DE} \sin(\vartheta_2) + r_{DCy})^2 + (r_{DE} \cos(\vartheta_2) + r_{DCx})^2} - l_{cyl}^0 + x_{cyl}^0 \quad (3.29)$$

Deriving the equation 3.29 above, as a function of the boom angle  $\vartheta_2$ , the piston velocity can be obtained:

$$\dot{x}_{cyl} = \frac{\delta x_{cyl}}{\delta \vartheta_2} \dot{\vartheta}_2 = \frac{\dot{\vartheta}_2 r_{DE} (r_{DCy} \cos(\vartheta_2) - r_{DCx} \sin(\vartheta_2))}{\sqrt{(r_{DE} \sin(\vartheta_2) + r_{DCy})^2 + (r_{DE} \cos(\vartheta_2) + r_{DCx})^2}} \quad (3.30)$$

### 3.1.5 Kinematic constraint

Once the dynamics for the vehicle structure has been defined, an additional *Kinematic constraint* is needed to complete the set of equations. The motivation is that, because of the boom motion around the point D, belonging to the chassis, a relative movement is present between the two bodies.

A material point that is moving on a plan, to which a coordinate system (x,y) is associated, can be located with a vector of position  $r$  defined as the vector drawn from the origin of the reference frame to the position P, that the point is occupying in the considered instant. In the considered case, a closed loop of position vectors can be built, from a defined global frame, whose origin is called O, to the axis of rotation, passing through D, connecting both bodies.

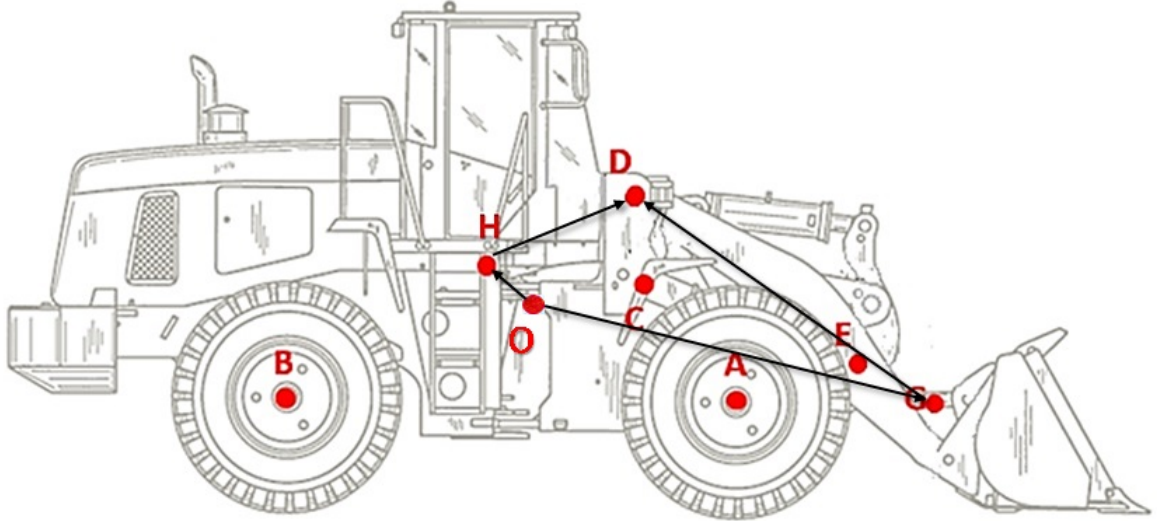


Figure 3.9: Kinematic constraint

$$r_{HO} + r_{DH} = r_{GO} + r_{DG} \quad (3.31)$$

Parameter	Complete expression
$r_{HOx}$	$-x_H$
$r_{HOy}$	$-y_H$
$r_{GOx}$	$x_G$
$r_{GOy}$	$y_G$

Table 3.2: Parameters expressions from global reference frame

In order to obtain the equations for the kinematic constraint of the body accelerations, the closed loop equation of the position vector has to be derived twice:

$$\begin{aligned} \ddot{x}_G = \ddot{x}_H - r_{DH} \cos(\vartheta_{DH} + \vartheta_1) \dot{\vartheta}_1^2 - r_{DH} \sin(\vartheta_{DH} + \vartheta_1) \ddot{\vartheta}_1 + \\ + r_{DG} \cos(\vartheta_{DG} + \vartheta_2) \dot{\vartheta}_2^2 + r_{DG} \sin(\vartheta_{DG} + \vartheta_2) \ddot{\vartheta}_2 \end{aligned} \quad (3.32)$$

$$\begin{aligned} \ddot{y}_G = \ddot{y}_H - r_{DH} \sin(\vartheta_{DH} + \vartheta_1) \dot{\vartheta}_1^2 + r_{DH} \cos(\vartheta_{DH} + \vartheta_1) \ddot{\vartheta}_1 + \\ + r_{DG} \sin(\vartheta_{DG} + \vartheta_2) \dot{\vartheta}_2^2 - r_{DG} \cos(\vartheta_{DG} + \vartheta_2) \ddot{\vartheta}_2 \end{aligned} \quad (3.33)$$

### 3.1.6 Equations derivation

Now that all the dynamic relationship have been defined, the final system equations can be obtained.

#### First equation

Combining the horizontal component of chassis and boom models (eq. 3.1 and eq. 3.4), and the one exploiting the relation between the actuator ends (eq. 3.23):

$$m_1\ddot{x}_H + m_2\ddot{x}_G = F_{Ax} + F_{Bx} \quad (3.34)$$

Then, including the horizontal equations that represent the forces applied to the wheels (eq. 3.19 and eq. 3.21):

$$m_1\ddot{x}_H + m_2\ddot{x}_G = -2k_{tx} - 2c_{tx} - k_{tx}(r_{AHy} + r_{BHy})\vartheta_1 - c_{tx}(r_{AHy} + r_{BHy})\dot{\vartheta}_1 + k_{tx}(x_{AR} + x_{BR}) + c_{tx}(\dot{x}_{AR} + \dot{x}_{BR}) \quad (3.35)$$

Eventually, adding the horizontal kinematic constraint of the body accelerations:

$$(m_1 + m_2)\ddot{x}_H - m_2r_{DHx}\ddot{\vartheta}_1 + m_2r_{DGx}\ddot{\vartheta}_2 = m_2r_{DHx}\dot{\vartheta}_1^2 - m_2r_{DGx}\dot{\vartheta}_2^2 - 2k_{tx}x_H - 2c_{tx}\dot{x}_H - k_{tx}(r_{AHy} + r_{BHy})\vartheta_1 - c_{tx}(r_{AHy} + r_{BHy})\dot{\vartheta}_1 + k_{tx}(x_{AR} + x_{BR}) + c_{tx}(\dot{x}_{AR} + \dot{x}_{BR}) \quad (3.36)$$

### Second equation

In order to obtain the second equation, the same procedure has to be applied, but, instead of combining the horizontal equations, the vertical components are utilized (eq. 3.2, eq. 3.5, eq. 3.24, eq. 3.20, eq. 3.22 and eq. 3.33):

$$m_1\ddot{y}_H + m_2\ddot{y}_G = F_{Ay} + F_{By} - m_1g - m_2g \quad (3.37)$$

$$\begin{aligned} m_1\ddot{y}_H + m_2\ddot{y}_G = & \\ -k_{ty}(y_H - y_{AR} + \vartheta_1 r_{AHx}) - c_{ty}(\dot{y}_H - \dot{y}_{AR} + r_{AHx}\dot{\vartheta}_1) - k_{ty}((y_H - y_{BR} - \vartheta_1 r_{BHx}) & \\ - c_{ty}(\dot{y}_H - \dot{y}_{BR} + r_{BHx}\dot{\vartheta}_1) - g(m_1 + m_2) & \end{aligned} \quad (3.38)$$

$$\begin{aligned} (m_1 + m_2)\ddot{y}_H + m_2 r_{DHx}\ddot{\vartheta}_1 + m_2 r_{DGx}\ddot{\vartheta}_2 = & \\ m_2 r_{DHx}\dot{\vartheta}_1^2 - m_2 r_{DGx}\dot{\vartheta}_2^2 - 2k_{ty}y_H - 2c_{ty}\dot{y}_H - k_{ty}(r_{AHx} + r_{BHx})\vartheta_1 & \\ - c_{ty}(r_{AHx} - r_{BHx})\dot{\vartheta}_1 + k_{ty}(y_{AR} + y_{BR}) + c_{ty}(\dot{y}_{AR} + \dot{y}_{BR}) - g(m_1 + m_2) & \end{aligned} \quad (3.39)$$

### Third equation

Starting from equation 3.3 and combining it with equations 3.4, 3.5, 3.23 and 3.24:

$$\begin{aligned} -m_2 r_{DHx}\ddot{x}_G + m_2 r_{DHx}\ddot{y}_G + J_1\ddot{\vartheta}_1 = & \\ F_{Ay}r_{AHx} + F_{Ax}r_{AHy} - F_{By}r_{BHx} + F_{Bx}r_{BHy} - F_{Ex}(r_{CHy} + r_{DHx}) + & \\ + F_{Ey}(r_{DHx} - r_{CHx}) - m_2 g r_{DHx} & \end{aligned} \quad (3.40)$$

Substituting the horizontal and vertical components of the boom center of gravity, obtained from the kinematic constraints (eq. 3.32 and eq. 3.33):

$$\begin{aligned}
& -m_2 r_{DH_y} \ddot{x}_H + m_2 r_{DH_x} \ddot{y}_H + [m_2(r_{DH_x}^2 + r_{DH_y}^2) + J_1] \ddot{\vartheta}_1 + \\
& \quad + m_2(r_{DH_x} r_{DG_x} - r_{DH_y} r_{DG_y}) \ddot{\vartheta}_2 = \\
& -m_2 r_{DH_y} r_{DH} \cos(\vartheta_{DH} + \vartheta_1) \dot{\vartheta}_1^2 + m_2 r_{DH_y} r_{DG} \cos(\vartheta_{DG} + \vartheta_2) \dot{\vartheta}_2^2 + \\
& + m_2 r_{DH_x} r_{DH} \sin(\vartheta_{DH} + \vartheta_1) \dot{\vartheta}_1^2 - m_2 r_{DH_x} r_{DG} \sin(\vartheta_{DG} + \vartheta_2) \dot{\vartheta}_2^2 + \\
& + F_{Ay} r_{AH_x} + F_{Ax} r_{AH_y} - F_{By} r_{BH_x} + F_{Bx} r_{BH_y} - F_{Ex} (r_{CH_y} + r_{DH_y}) + \\
& \quad + F_{Ey} (r_{DH_x} - r_{CH_x}) - m_2 g r_{DH_x} \quad (3.41)
\end{aligned}$$

Eventually, to gain the third equation, the above equation has to be combined with 3.19, 3.20, 3.21 and 3.22, from the wheels model, 3.25 and 3.26, from the hydraulic actuator geometry:

$$\begin{aligned}
& -m_2 r_{DH_y} \ddot{x}_H + m_2 r_{DH_x} \ddot{y}_H + [m_2(r_{DH_x}^2 + r_{DH_y}^2) + J_1] \ddot{\vartheta}_1 + \\
& \quad + m_2(r_{DH_x} r_{DG_x} - r_{DH_y} r_{DG_y}) \ddot{\vartheta}_2 = \\
& \quad + m_2 r_{DH_y} r_{DG_x} \dot{\vartheta}_2^2 - m_2 r_{DH_x} r_{DG_y} \dot{\vartheta}_2^2 - c_{tx} (r_{AH_y} + r_{BH_y}) \dot{x}_H + \\
& + c_{ty} (r_{BH_x} - r_{AH_x}) \dot{y}_H + [-c_{tx} (r_{AH_y}^2 + r_{BH_y}^2) - c_{ty} (r_{AH_x}^2 + r_{BH_x}^2)] \dot{\vartheta}_1 + \\
& \quad - k_{tx} (r_{AH_y} + r_{BH_y}) x_H + k_{ty} (r_{BH_x} - r_{AH_x}) y_H + \\
& \quad + [-k_{tx} (r_{AH_y}^2 + r_{BH_y}^2) - k_{ty} (r_{AH_x}^2 + r_{BH_x}^2)] \vartheta_1 + \\
& \quad + F_{cyl} [-\sin(\gamma) (r_{DH_x} - r_{CH_x}) - \cos(\gamma) (r_{DH_y} + r_{CH_y})] + \\
& + k_{tx} r_{AH_y} x_{AR} + c_{tx} r_{AH_y} \dot{x}_{AR} + k_{ty} r_{AH_x} y_{AR} + c_{ty} r_{AH_x} \dot{y}_{AR} + k_{tx} r_{BH_y} x_{BR} + \\
& \quad + c_{tx} r_{BH_y} \dot{x}_{BR} - k_{ty} r_{BH_x} y_{BR} - c_{ty} r_{BH_x} \dot{y}_{BR} - m_2 r_{DH_x} g \quad (3.42)
\end{aligned}$$

### Fourth equation

With the same procedure adopted for reaching the third equation, starting from eq. 3.6 and adding the equations 3.4, 3.5, 3.25, 3.26, and 3.32, 3.33, the last equation of the vehicle dynamics can be achieved:

$$\begin{aligned} m_2 r_{DGy} \ddot{x}_H + m_2 r_{DGx} \ddot{y}_H + m_2 (r_{DHx} r_{DGx} - r_{DHy} r_{DGy}) \ddot{\vartheta}_1 + \\ + [J_2 + m_2 (r_{DGy}^2 + r_{DGx}^2)] \ddot{\vartheta}_2 = \\ + m_2 r_{DHy} \dot{\vartheta}_1^2 - m_2 r_{DGy} \dot{\vartheta}_2^2 + m_2 r_{DHx} \dot{\vartheta}_1^2 - m_2 r_{DGx} \dot{\vartheta}_2^2 + \\ + F_{cyl} [-\sin(\gamma)(r_{DGx} - r_{EGx}) + \cos(\gamma)(r_{DGy} - r_{EGy})] - m_2 r_{DGx} g \end{aligned} \quad (3.43)$$

## 3.2 Hydraulics

Since the objective of the research is to reduce the machine oscillations taking advantage of the boom movements, to model the hydraulics, I focused on the lift cylinders behavior:

- what is the effect of their motion on the rest of the vehicle,
- how disturbances directly acting on the wheels can influence the implement,
- how the hydraulic supply affects their dynamics.

### 3.2.1 Hydraulic actuator

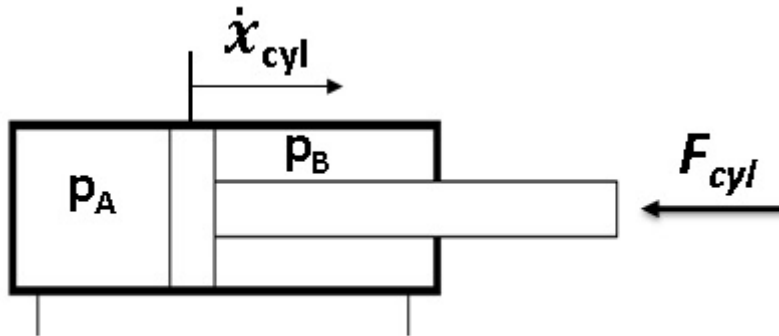


Figure 3.10: Asymmetric linear actuator

When the piston is stretching out, the force balance equation can be written as:

$$m_p \ddot{x}_{cyl} = -f_V \dot{x}_{cyl} + (A_A - f_C) p_A - A_B p_B - F_{cyl} \quad (3.44)$$

- $m_p$  piston mass,
- $A_A$  area of A flat piston side,
- $A_B$  area of B rod side,
- $p_A$  pressure inside A flat piston chamber,
- $p_B$  pressure inside B rod chamber,
- $f_V$  viscous friction coefficient,
- $f_C$  Columbus friction coefficient,
- $\dot{x}_{cyl}$  piston velocity,
- $\ddot{x}_{cyl}$  piston acceleration,
- $F_{cyl}$  external load force.

Among them, for the project purpose, the two friction coefficients have a very low impact, when compared to the other entities in the equation.  $F_{cyl}$  represents the force introduced by the boom, which, being stressed in the points where it is conjuncted with the chassis, induces a pressure variation in the cylinder chambers.

Besides, from the flow continuity equation applied to the actuator, it can be derived that:

$$\dot{p}_A = \frac{1}{C_{HA}}(Q_{IN} - A_A \dot{x}_{cyl} - 2k_{Li}(p_A - p_B)) \quad (3.45)$$

$$\dot{p}_B = \frac{1}{C_{HB}}(-Q_{OUT} + A_B \dot{x}_{cyl} + 2k_{Li}(p_A - p_B)) \quad (3.46)$$

In the equations above  $k_{Li}$  represents an internal leakage coefficient, while  $C_{HA}$  and  $C_{HB}$  are respectively equal to  $V_A/B_A$  and  $V_B/B_B$ .

$$V_A = V_A^0 + A_A x_{cyl} \quad (3.47)$$

$$V_B = V_B^0 - A_B x_{cyl} \quad (3.48)$$

The parameters  $V_{A/B}$  are the volumes from each side of the piston, and they are composed by a constant component  $V_{A/B}^0$ , that is the total chamber volume, including the pipes supplying the actuator, plus a variable part dependent on the piston position with respect to the nominal one.

$B_{A/B}$  are the Bulk modulus of the two chambers:

$$B = -V \frac{dp}{dV} \quad (3.49)$$

This parameter reflects the incompressibility of the fluid, it is pressure dependent, but is usually assumed to be constant when the range of operating pressures is limited.

### 3.2.2 Supply dynamics

In order to make the boom move, as suggested by the equations related to the hydraulic cylinder, reported in the previous subsection, a certain amount of flow rate is needed. In the analyzed machine, the hydraulic supply corresponds to a variable displacement load sensing pump.

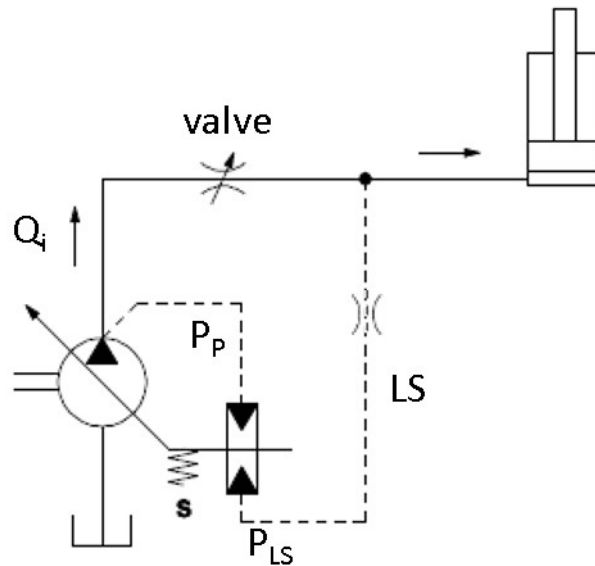


Figure 3.11: Simplified hydraulic schematic

The simplified circuit, in figure 3.11, reports the basic principle of the load sense (LS), applied to a system close enough to the one present on the wheel loader. The pressure, coming from the line supplying the load, sets the displacement of the pump, by abiding the following force balance equation:

$$P_P A_P = P_{LS} A_{LS} + F_s \quad (3.50)$$

The force, corresponding to the pressure on the load sense line  $P_{LS}$ , applied to a specific constant area  $A_{LS}$ , summed with the force derived by a spring, with a variable previously selected winding, has to be balanced by the force coming from the pressure of the pump  $P_P$  acting on a constant area  $A_P$ . In such a way, depending on the load, the pump will deliver more or less flow rate.

After the flow has been sent from the pump, it has to be directed into different cylinder chambers, depending on whether the required action is to extend or retract the piston. The element utilized to accomplish this job is a directional valve.

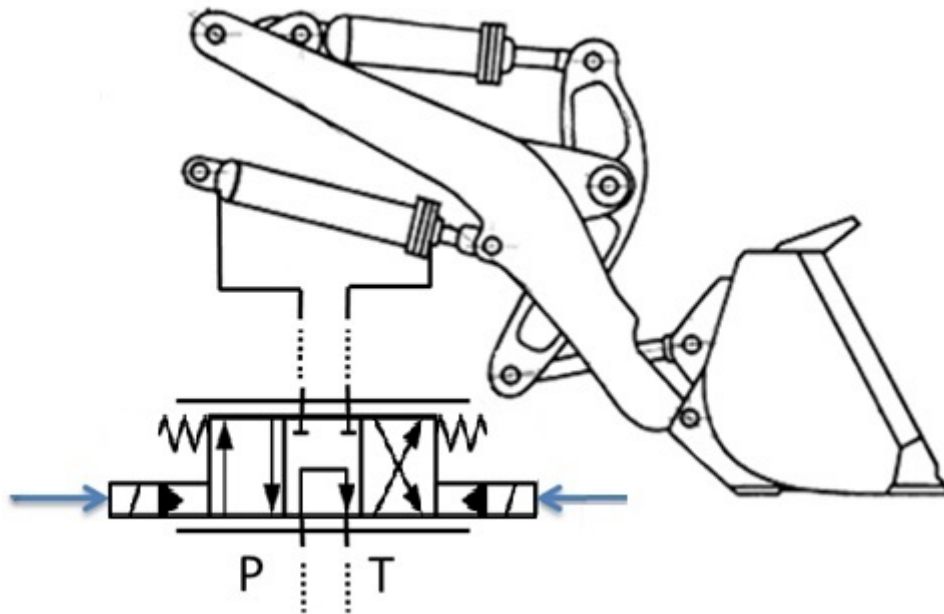


Figure 3.12: Simplified schematic of directional valve and implement

A proportional directional valve is mounted on the studied vehicle. The valve is composed by pilot and main stage. Thanks to the first one, the user can decide direction and flow rate, by varying signal applied to the pilot stage. For moving the boom, the user can act on an hydraulic command or on an electro-hydraulic one. With both of them the two parameters can be changed. Signal and opening of the spool are proportional: the higher is the pilot signal, the greater is the section through which the flow can pass.

The main stage, instead, is formed by multiple positions. The flow goes across one of them and it is directed to a certain actuator chamber and to tank, depending on the pilot signal entity.

In order to model pump and proportional directional valve dynamics, the system has been previously tested. The experiment was characterized by the motion of the implement, commanded by various input signals, different in amplitude and frequency. Multiple data, among which boom angle, pilot and actuator pressures, has been taken and collected. Those values has been used to obtain the parameters necessary to compose a transfer function, able to correctly describe the supply dynamic behavior.

$$\frac{K\omega_n^2}{s^2 + 2\zeta\omega_n s + \omega_n^2} \quad (3.51)$$

### 3.3 Complete model

Once all the sub-models have been deduced, they have to be combined for obtaining the complete structure:

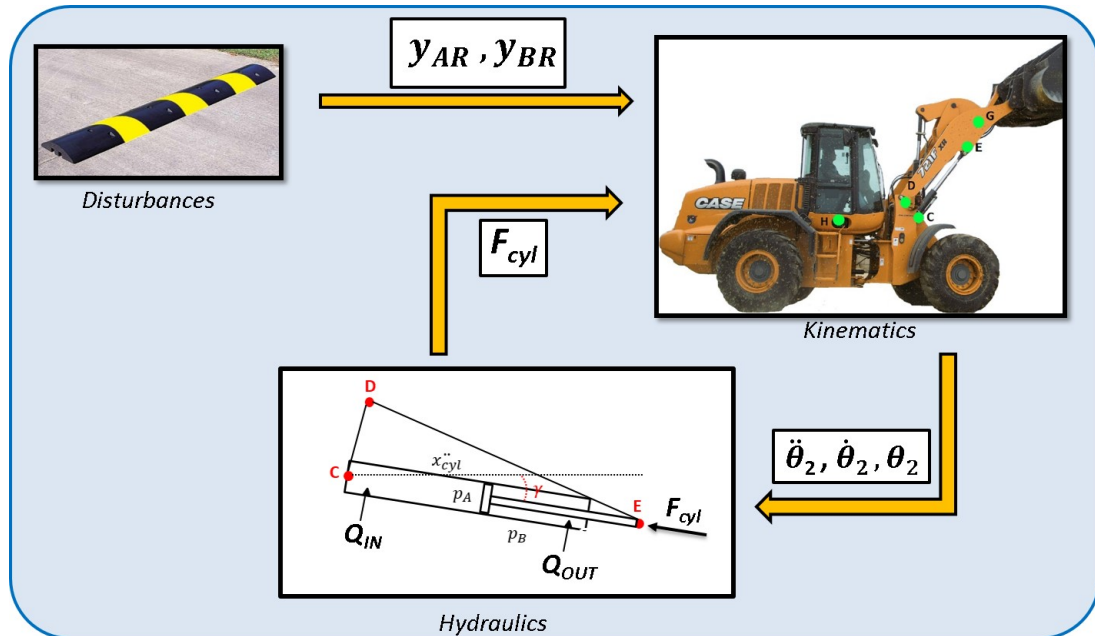


Figure 3.13: Schematic of the model structure

The *Vehicle dynamic* model is influenced by time variant road *Disturbances*. The uneven street produces a modification of the vehicle variables. The forces applied make the boom move and, for this reason, position, velocity and acceleration of the arm change. An implement motion induces a variation of piston variables and pressure inside the hydraulic actuator chambers and therefore, it causes an alteration of the force  $F_{cyl}$  applied to the piston. This stress then spreads to the vehicle again, dynamically changing the system behavior.

The complete set of equations has been implemented through *Simulink* blocks and with *Matlab* code and logic. After some debugging action to obtain the correct simulation, the model has been compared and validated with respect to the real machine behavior.

### 3.4 Model validation

In order to correctly validate the model, some requirements on the experimental procedure have to be defined:

Firstly, the test have to induce enough stress to the system, so that appreciable results in oscillations can be seen.

Then, it has to be repeatable, in a manner that it can be done multiple times without drastic modifications in the outcome.

Lastly, to see if the model properly follows the reality, the system has to be tested in different scenarios. Hence, more than one test has to be performed.

To comply with the requirements, multiple tests have been executed. The basis of the procedure is always the same, riding the wheel loader until a speed bump is hit. The reason why this element of driving disturbance has been chosen is that the road profile excursion is always the same. This devices have been traversed at different vehicle velocity and boom inclination. But, since the final results where really close, when changing the implement angle or over a certain speed, only two test cases will be shown:

1. speed bump at low speed
2. speed bump at high speed

In both cases, the main parameters to be checked are the cabin vertical acceleration and the differential pressure  $\Delta P$  inside the cylinders. When hitting a speed bump on a real vehicle, variations on the measurements of the boom angle  $\vartheta_2$  are not perceptible, since they are hidden by electrical noise. The simulation results will be presented anyway, to show their entity.

In the following figures, the vertical axis represents the variable, while the horizontal refers to the time. The red continuous lines are the simulation results and the dotted blue lines the experimental data.

### 3.4.1 Case 1

In the first test, the vehicle hit a speed bump when it is on the first gear, at the maximum speed. After some meters of acceleration, the machine reaches a cruise constant velocity, making the test reliable and repeatable. In the behavior of the vehicle variables, it is noticeable the presence of two major peaks: the first one related to the front wheels hitting the speed bump and the second one to the rear wheels.

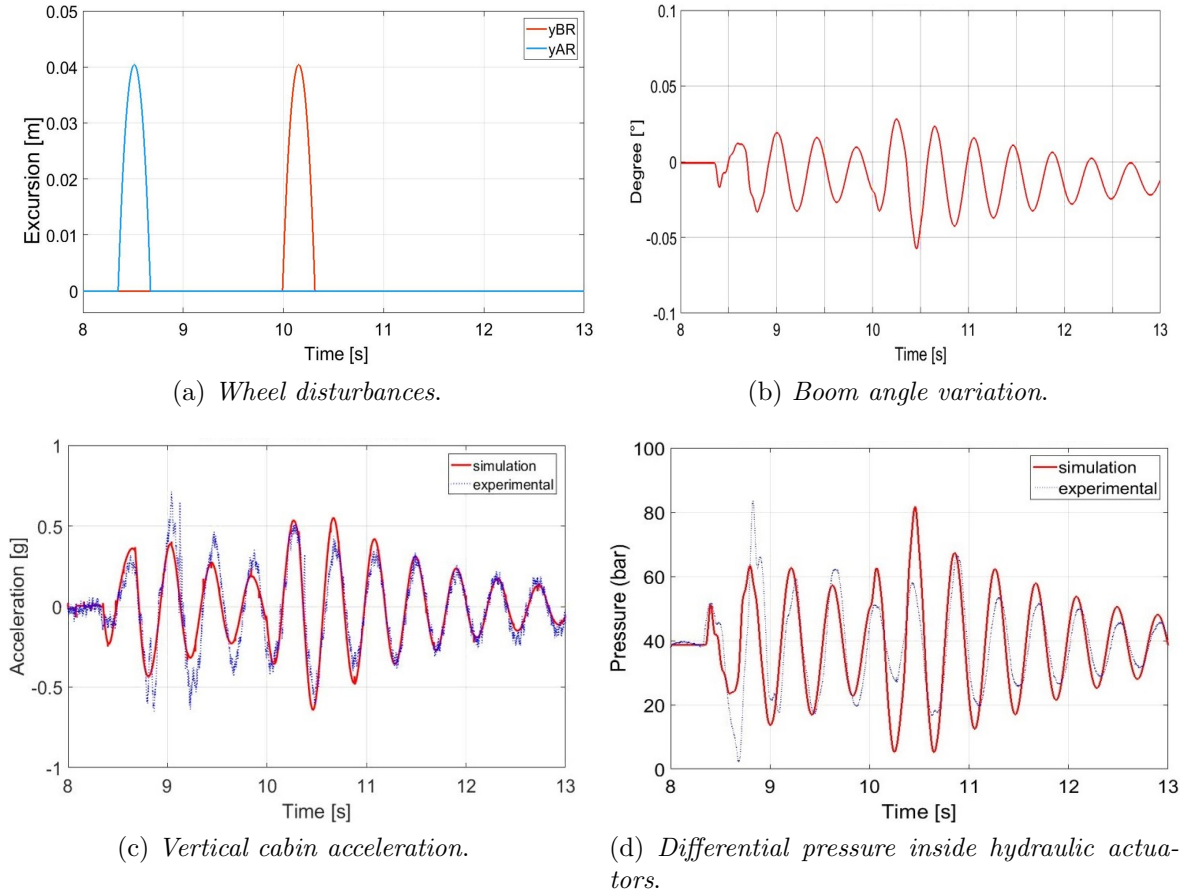


Figure 3.14: First test case validation results

As clear from the figure 3.14 above, the shapes of the two cabin acceleration lines are really close, in both frequency and amplitude.

Other than acceptable discrepancies, the behavior of the pressure in the actuators for the experimental collected data is well matched by the model simulation result.

Besides, as previously pointed out, because of the electric noise, coming from the sensors, the boom angle variation is too limited to make an appreciable comparison between model and reality. Anyways, it can be seen, that there is a slight tendency of the boom to be lowered when subject to big pressure oscillation.

### 3.4.2 Case 2

As in the first case, the vehicle has to hit the speed bump at a constant velocity. The only difference is that, in the second case, since the wheel loader is pushed at its maximum velocity on the second gear, the reached vehicle speed is higher. For this reason, the behavior of the curves is different: the two main peaks are closer, since the time interval, between front and rear wheels passing over the bump, is smaller; and the amplitude of the induced oscillations is higher. While the real machine always has small vibrations, caused by a slight uneven road, the simulated model has no wheel displacement variation other than the speed bump. For this reason, it must be noted that, in the following figures, before the defined instant, in which the front wheels hit the hump, the variable simulation values are flat.

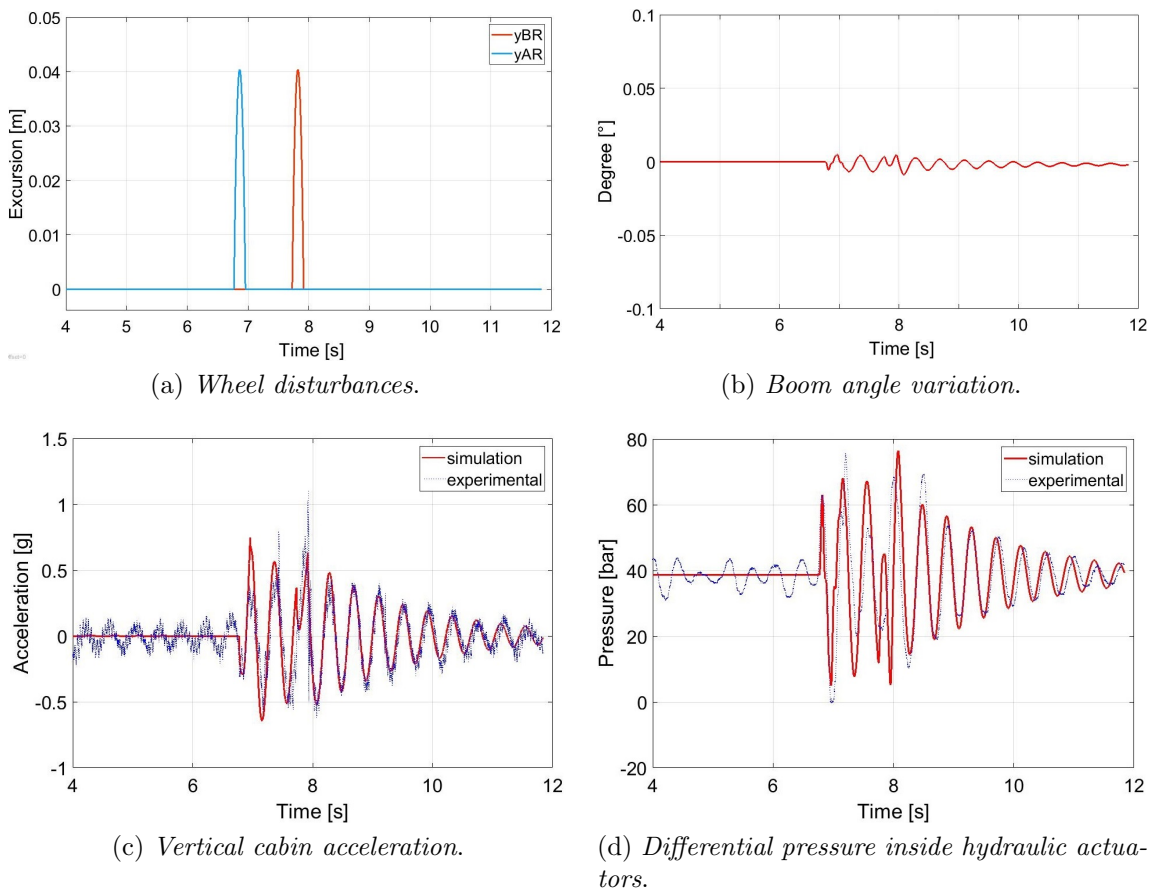


Figure 3.15: Second test case validation results

# Chapter 4

## Control strategy

In this chapter, it will firstly be presented a comparison between different control structures, based on the results coming from past effort. After that, multiple signals, as feedback choice, will be shown. At the end, the model simulation results will be summarized and commented.

### 4.1 Control structure

As previously anticipated, because of the lack of suspensions on the wheels, one of the few methods, for reducing this type of vehicle cabin oscillations, is to control the hydraulic lift actuators. This command allows to obtain a movement of the arm, such that it can be feasible to balance this negative phenomenon.

Using the boom motion, in the past, different control structures have been applied with the goal of bounding the vehicle oscillations. Someone decided to solve the problem using the boom and cabin accelerations, as feedback signals, passing through complex control structures, managing the signal adaptively or building the controller with robust design methods.

For different reasons, such as difficulties in the transition from simulation parameters to reality or in the implementation of the controller logic on an electronic device or because of a restricted effectiveness in some working conditions, all these complicated techniques have had a limited outcome on the actual vehicle, hence the results were not as good as expected.

The purpose of this research, in fact, has been to design a simple controller and find an easy strategy, suitable for the application, able to be sufficiently effective in every possible situation.

For this reason, thanks to past work on oscillation reduction for hydraulic actuators, the final decision on the control structure has been a simple filter, with the task of processing signals, coming from the sensors present on the wheel loader, to give a proper command to the proportional directional valve and therefor to move the boom.

## 4.2 Feedback choice

Once the structure has been defined, the main remaining option is on the selection of the best feedback signal. On the simulated model, every variable can be selected, while on the real machine data of some parameter can not be collected, for both difficulty in mounting operation and cost of equipment. The wide range of possibility narrows down when considering only useful signals. For this reason, all the parameters with behavior not close enough with respect to the cabin oscillations have to be removed from the list of possible feedback choice. Since the boom angle motion is not appreciable, it has to be ruled out too.

The most reasonable choices remain the vertical cabin acceleration, parameter whose oscillations have to be reduced, and the pressure inside the lift cylinders, since an option through which the vehicle vibrations can be reduced is with the actuator movement.

The project approach is founded on commanding the movements of the lifting boom actuators, hence the hydraulic system, with the objective of reducing the cabin oscillations, inside which the driver seats.

Using a model-based approach, to calculate the control parameters, the model has to be perfectly known. Using the vertical cabin acceleration variable as the feedback signal, it means that the complete system, with many complex equations and including all the non-linearities, has to be considered as the plant model the controller has to deal with.

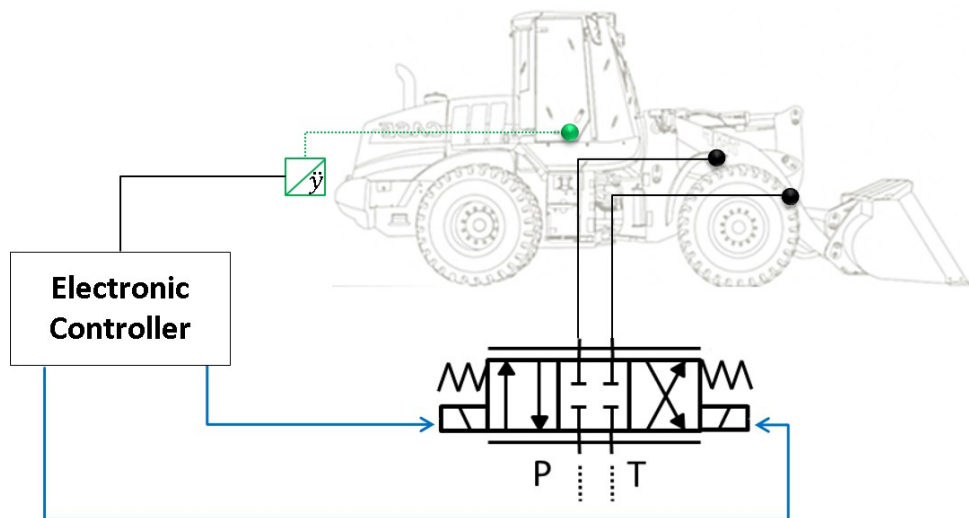


Figure 4.1: Schematic of the acceleration feedback control structure

As a consequence, the correct control algorithm would become difficult to obtain.

Choosing the pressure inside the actuators, instead, makes the control easier to be implemented. The plant, in fact, can be simplified, from the complete vehicle model to the hydraulic part. The parameters of the hydraulics would obviously remain the same, while the force applied to the piston, thus the boom weight and dynamic, would be simulated as an external disturbance.

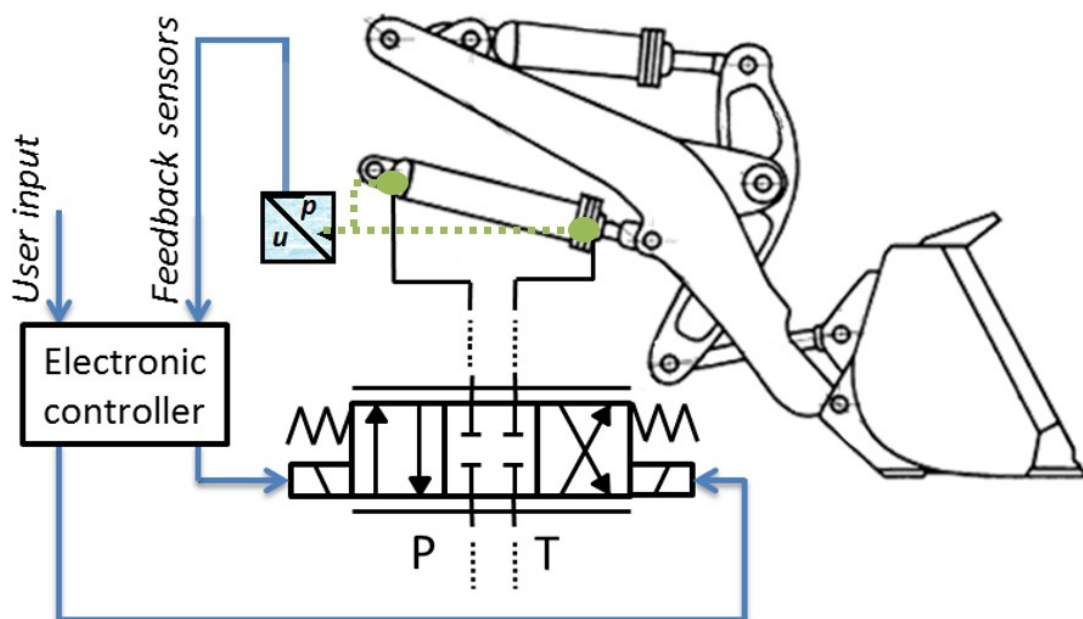


Figure 4.2: Applied schematic of the pressure feedback control logic

### 4.3 Controller design

Once the feedback choice has been made, the plant model has to be obtained. The objective is to have a unique transfer function, whose output is the differential pressure inside the cylinders, and whose input is the flow coming from the hydraulic supply.

#### 4.3.1 Plant model deduction

Starting from the deduced model for the hydraulics of the vehicle, on Chapter 3.2, assuming the internal leakage contribution negligible, it can be stated that the Laplace transformed equations produce:

$$p_A = \frac{1}{sC_{HA}}(Q_{IN} - A_A\dot{x}_{cyl}) \quad (4.1)$$

$$p_B = \frac{1}{sC_{HB}}(-Q_{OUT} + A_B\dot{x}_{cyl}) \quad (4.2)$$

$$m_p v s = -f_V v + A_A p_L - F_{cyl} \quad (4.3)$$

Where  $m_p$  corresponds to the mass of the piston and  $v$  to its velocity. Being the system provided of asymmetric cylinders,  $p_L$  represents the load pressure, therefor the differential pressure in the actuator chambers, and  $\alpha = A_B/A_A$  is the area ratio.

It can also be written that:

$$p_L = p_A - \alpha p_B \quad (4.4)$$

$$Q_B = \alpha Q_A \quad (4.5)$$

$$A_B = \alpha A_A \quad (4.6)$$

Then, from the equation above, another way to write  $p_L$  is:

$$p_L = \frac{1}{s}(Q_A - A_A)\left(\frac{1}{C_{HA}} + \frac{\alpha^2}{C_{HB}}\right) \quad (4.7)$$

From equation 4.3, the piston velocity can be made explicit:

$$v = \frac{p_L A_A - F_{cyl}}{m_p s + f_v} \quad (4.8)$$

For simplifying the following notations:

$$O = \frac{1}{C_{HA}} + \frac{\alpha^2}{C_{HB}} \quad (4.9)$$

Combining equations 4.7 and 4.8, for the linearity condition and the superposition principle, the output, load pressure  $p_L$ , can be rewritten as a function of the input, flow rate  $Q_A$ , with the addition of a disturbance, the force applied to the piston  $F_{cyl}$ :

$$p_L = \frac{(m_p s + f_v)O}{m_p s^2 + f_v s + A_A^2 O} Q_A + \frac{A_A O}{m_p s^2 + f_v s + A_A^2 O} F_{cyl} \quad (4.10)$$

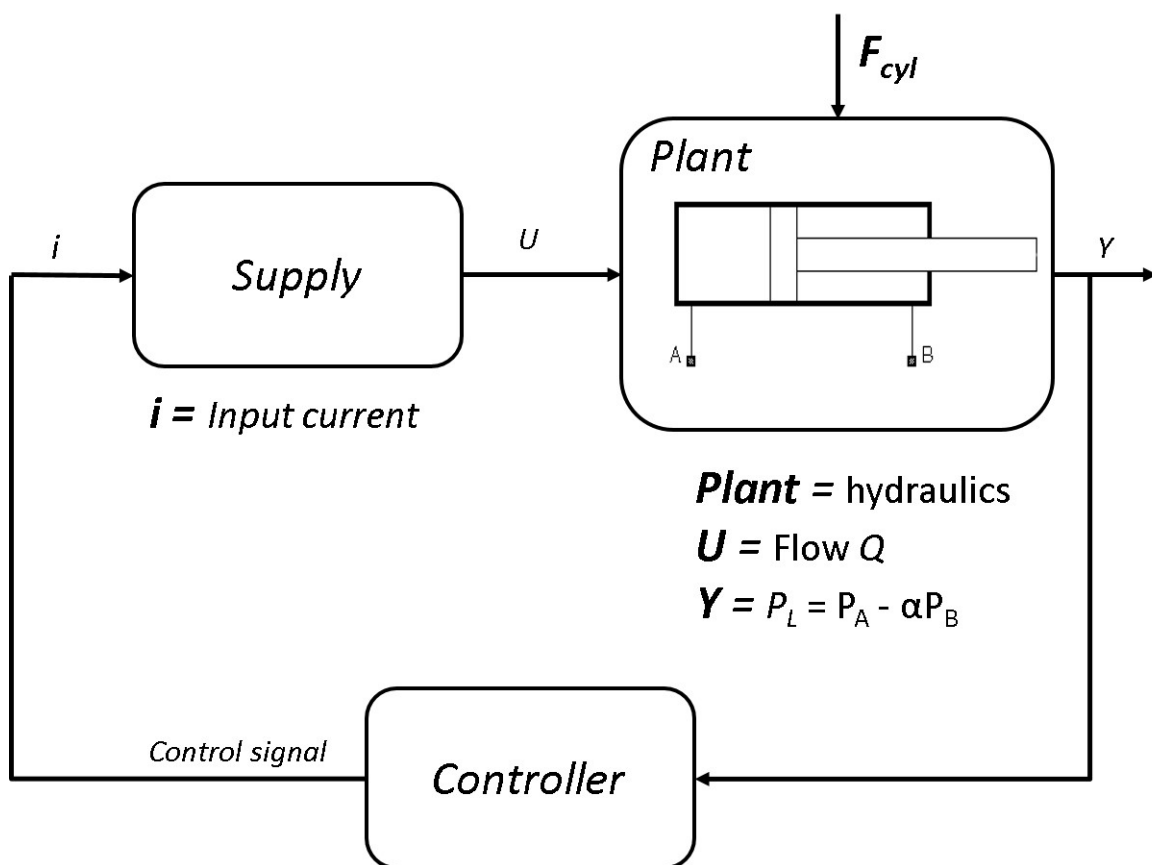


Figure 4.3: Schematic of the pressure feedback control structure

### 4.3.2 Filter implementation

As a controller function, for the easiness of the project, a filter has been implemented. In the first step, toward the control parameters deduction, the supply dynamics and therefor the valve implementation is excluded. Their contribution will be introduced afterwards. Hence, what remains is the hydraulic model and the electronic controller.

The plant transfer function can be thus written on the standard form:

$$G(s) = \frac{y(s)}{u(s)} = \frac{Kw_n^2}{s^2 + 2\zeta w_n s + w_n^2} \quad (4.11)$$

Where  $K$  is the gain,  $w_n$  the natural frequency and  $\zeta$  the damping ratio.

The purpose of the control action is to reduce the oscillations of the system, hence, to increase the value of the damping ratio. To obtain this objective, an addition gain has to be introduced. But, since a simple gain could lead to affect not only the damping factor, but also the steady state gain and the natural frequency, a filter is often needed.

For the active damping approach, applied to hydraulic systems, past literature suggests the use of high pass (HP) or low pass (LP) filters as the most effective ways to reduce oscillations of the actuators. For this reason, I decided to implement both of them in order to see benefits and drawbacks of the two strategies.

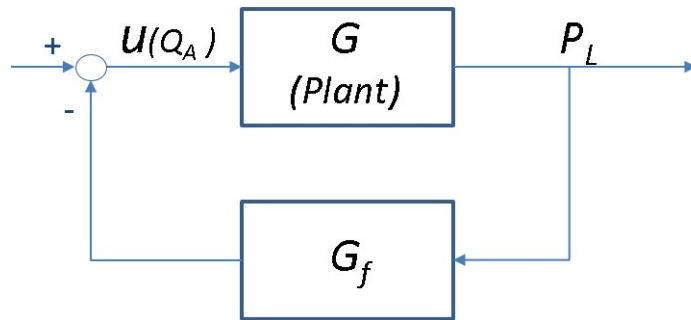


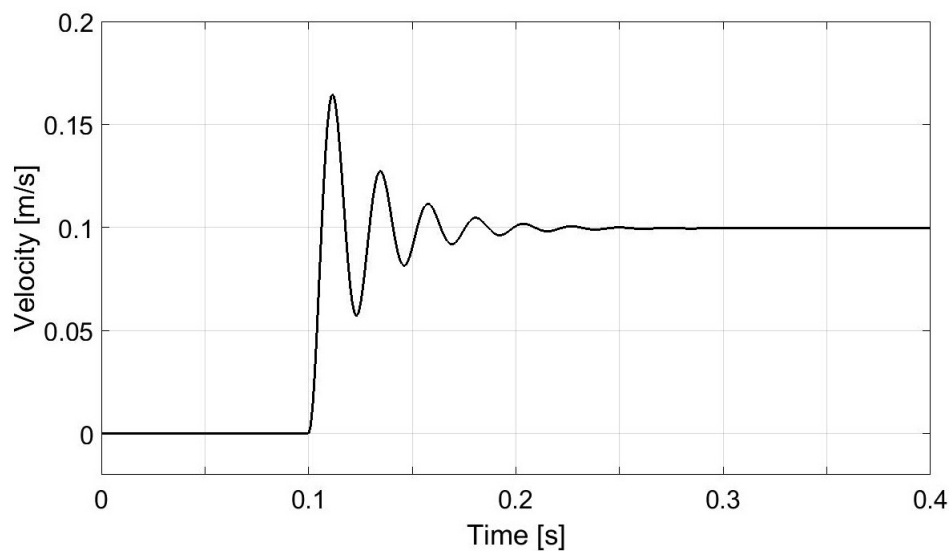
Figure 4.4: Simplified schematic of the control structure

In order to compare the different filter oscillation reduction, a commanded piston speed will be requested. The resulting velocity and pressure load, with respect to the mean value, will be figured to show the improvements of the control algorithms.

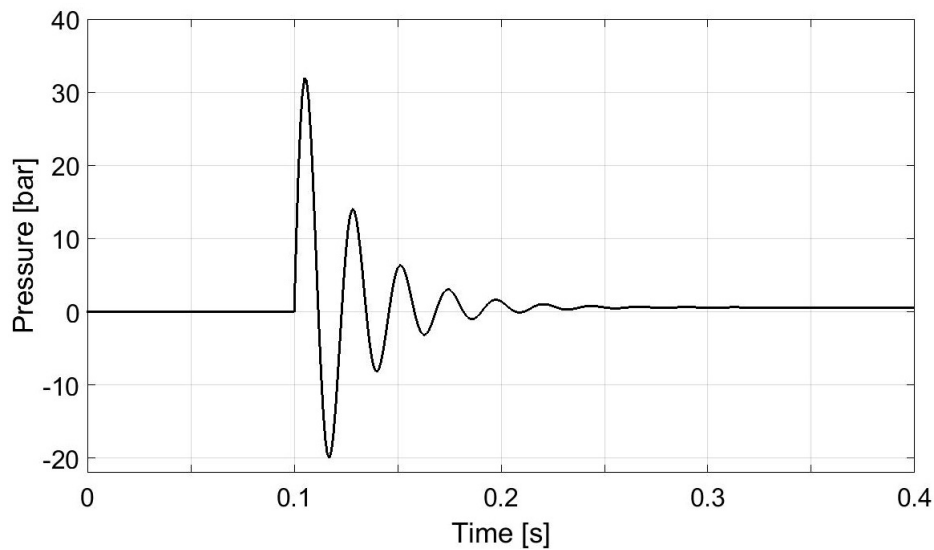
Considering the flow rate  $Q$  as the only input of the model, with a disturbance  $F_{\text{cyl}}$  approximated to a constant value, the plant transfer function is:

$$G(s) = \frac{p_L(s)}{Q_A(s)} = \frac{(m_p s + f_v)O}{m_p s^2 + f_v s + A_A^2 O} \quad (4.12)$$

When no controller is applied, the simulation results are the following:



(a) *Piston velocity.*



(b) *Pressure load.*

Figure 4.5: Simulation results for test without control

As clear from the figures, oscillations of big amplitude are present. Besides, it must be noted that the value 0 of the  $P_L$  corresponds to the mean value that the pressure load has, before the alteration, caused by the input variation.

### Low Pass Filter

The low pass filter transfer function can be described as:

$$G_f(s) = \frac{K_f}{\tau s + 1} \quad (4.13)$$

Where  $K_f$  is the filter gain and  $\tau$  is the time constant.

By varying the two filter variables, different results can be achieved. There clearly is a close relationship between them. But, to reach the optimal damping performance, their values have to be properly selected. It is almost impossible to directly obtain an analytical equation, able to correctly link them, so that the oscillation reduction is maximized.

Instead, a *Root Locus* plot technique has been used:

as the method suggests, for understanding the effect of one parameter on the system, the structure has to be transformed in the standard form. This means that only a gain, in this case  $K_f$ , is present on the feedback line.

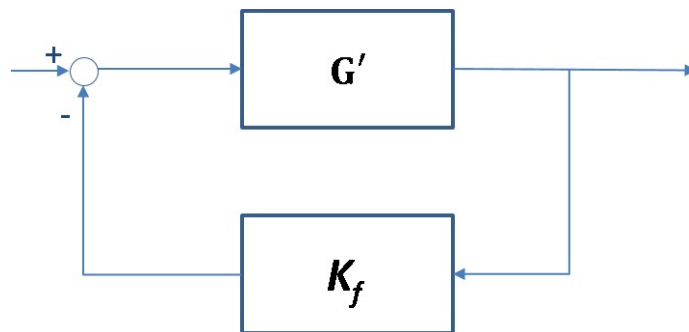


Figure 4.6: Structure modification for root locus method

Respecting the root locus rule, the plant transfer function is modified as follows:

$$G'(s) = \frac{(m_p s^2 + f_v s)O}{m_p \tau s^3 + (f_v \tau + m_p) s^2 + (A_A^2 O \tau + f_v) s + A_A^2 O} \quad (4.14)$$

The method used to find the optimal correlation between the two parameters  $K_f$  and  $\tau$ , such that the resultant damping ratio is higher, has been to plot multiple times the root locus of the plant transfer function, keeping the value of  $\tau$  constant, on each simulation, and varying the one of  $K_f$ .

The resulting expression is then rewritten in the standard form  $1 + K_f G'(s) = 0$ :

$$1 + K_f \frac{(m_p s + f_v)O}{m_p \tau s^3 + (f_v \tau + m_p) s^2 + (A_A^2 O \tau + f_v) s + A_A^2 O} = 0 \quad (4.15)$$

The result is shown in the following figure:

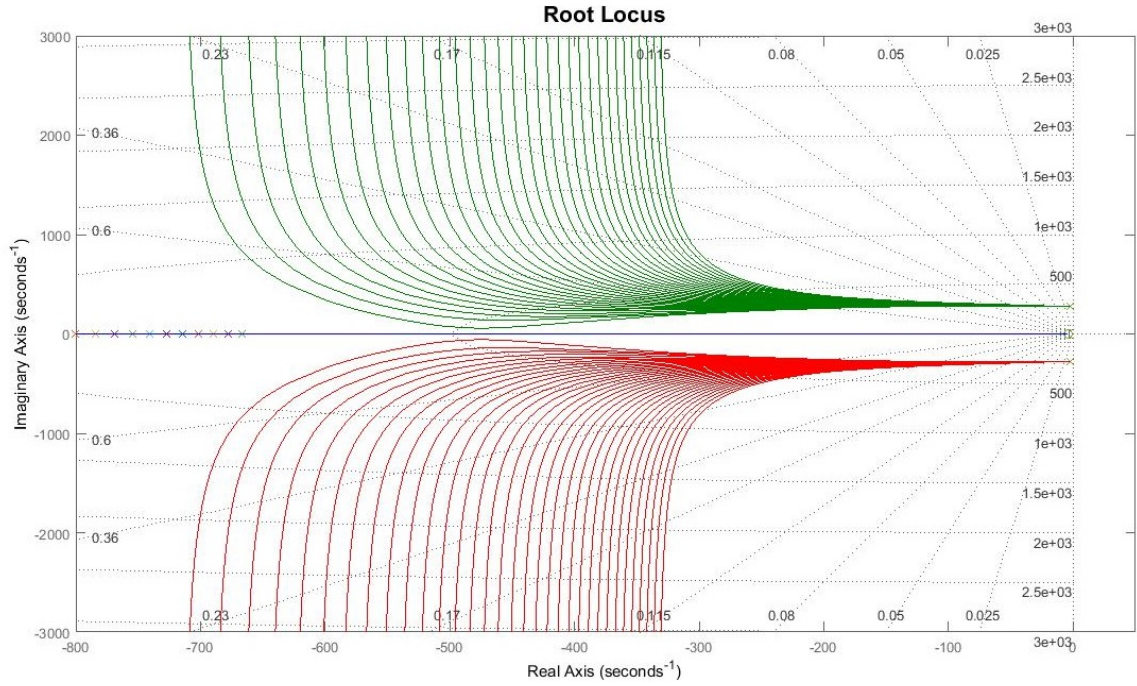


Figure 4.7: Root locus plot with LP filter, when  $\tau$  is constant on each curve and  $K_f$  varies

The two axes represent Real and Imaginary values of the curves. The curved lines correspond to the natural frequency  $w_n$ , while the straight lines are the damping ratio  $\zeta$ . The plot is symmetrical with respect to the horizontal axis, that also represents damping ratio equal to 1. In fact,  $\zeta$  is equal to 0 starting from the vertical line, and proceeding counterclockwise until the maximum value 1.

Since the objective of the technique is to reach the highest  $\zeta$  possible, the closest curve to the horizontal axis has to be selected. After that, picking the optimal point on the curve, it reveals the related value of  $K_f$ . In the studied case, the lower the value of  $\tau$  the closer the curve is with respect to the Real Axis.

Applying the LP filter to the structure, the results to the previously decided test procedure are the following:

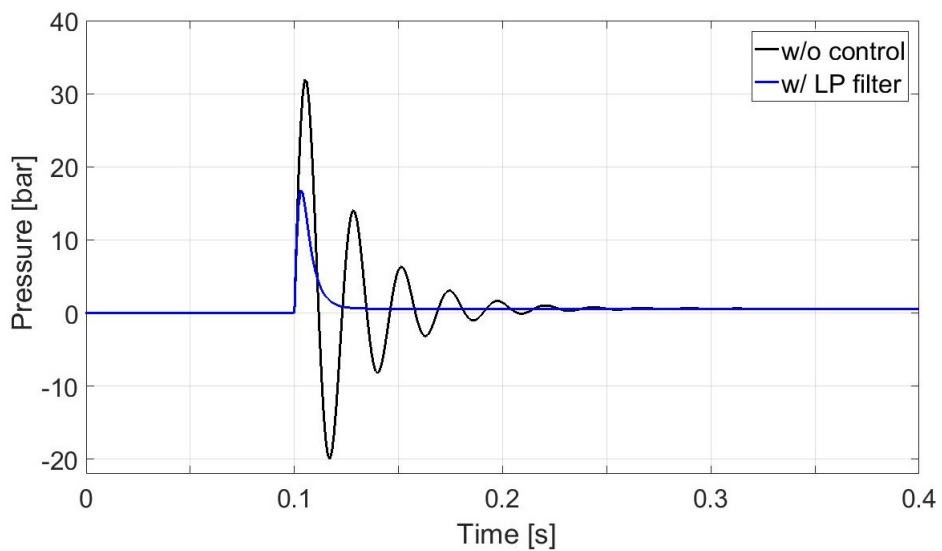
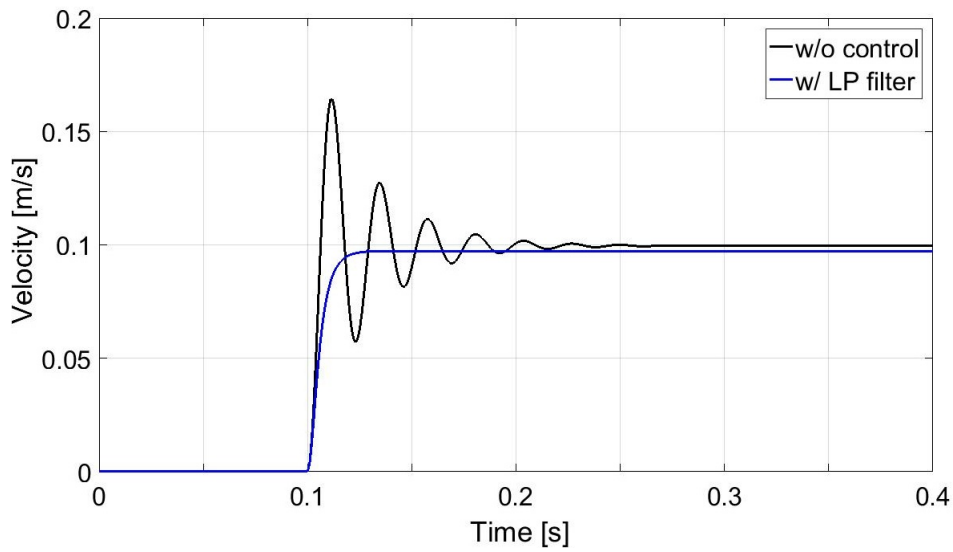


Figure 4.8: Comparison of simulation results with LP filter applied and not

The oscillation reduction is evident in both piston velocity and pressure load. The only limiting response is that the actuator speed is not exactly the one commanded, but there is a steady-state error.

## High Pass Filter

The high pass filter transfer function can be written as:

$$G_f(s) = \frac{K_f s}{\tau s + 1} \quad (4.16)$$

Where  $K_f$  is the filter gain and  $\tau$  is the time constant.

As for the low pass filter, the plant model has to be modified, in a similar manner, to obtain a direct expression on how the feedback gain affect the system. The equation is written in the standard form and the result is:

$$1 + K_f \frac{(m_p s^2 + f_v s) O}{m_p \tau s^3 + (f_v \tau + m_p) s^2 + (A_A^2 O \tau + f_v) s + A_A^2 O} = 0 \quad (4.17)$$

The figure, showing the different plant transfer function curves, varying  $K_f$  with  $\tau$  constant for each of them, is:

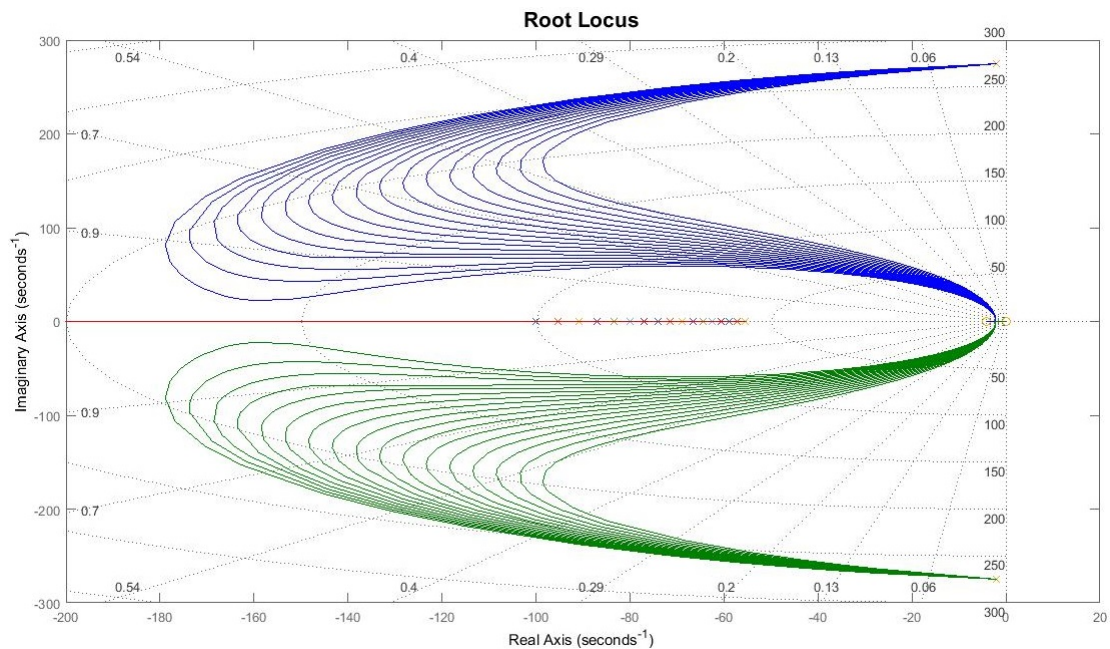
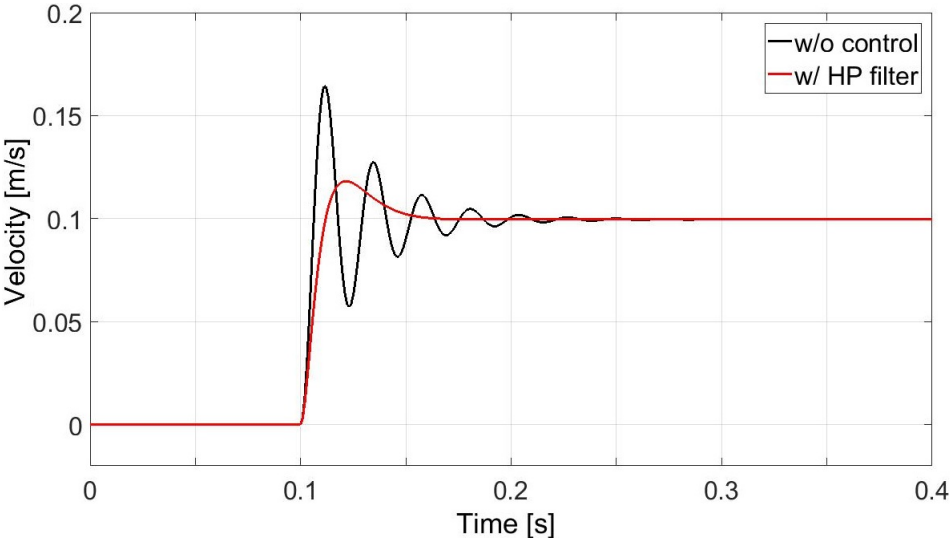


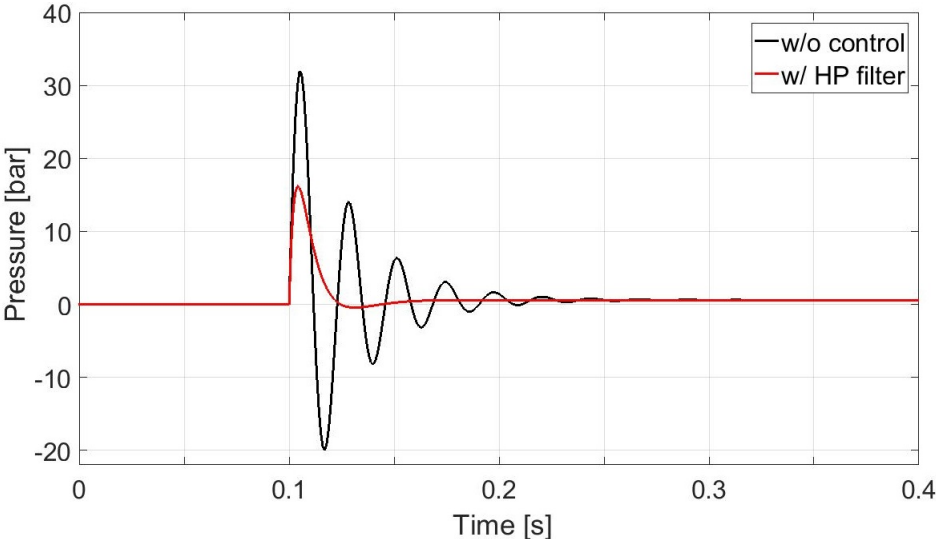
Figure 4.9: Root locus plot with HP filter, when  $\tau$  is constant on each curve and  $K_f$  varies

The root locus plot has already been described and the followed procedure, used to find the two parameters in an optimal configuration, is the same utilized for the low pass filter case. The only difference is that, while for the other filter, increasing the value of  $\tau$  means decreasing the reachable damping ratio, here, the higher is the time constant, the closer the curve is to the horizontal axis.

Once the filter is applied in the control structure, the comparison between the models, with and without high pass filter, is shown in the figures below:



(a) Piston velocity.



(b) Pressure load.

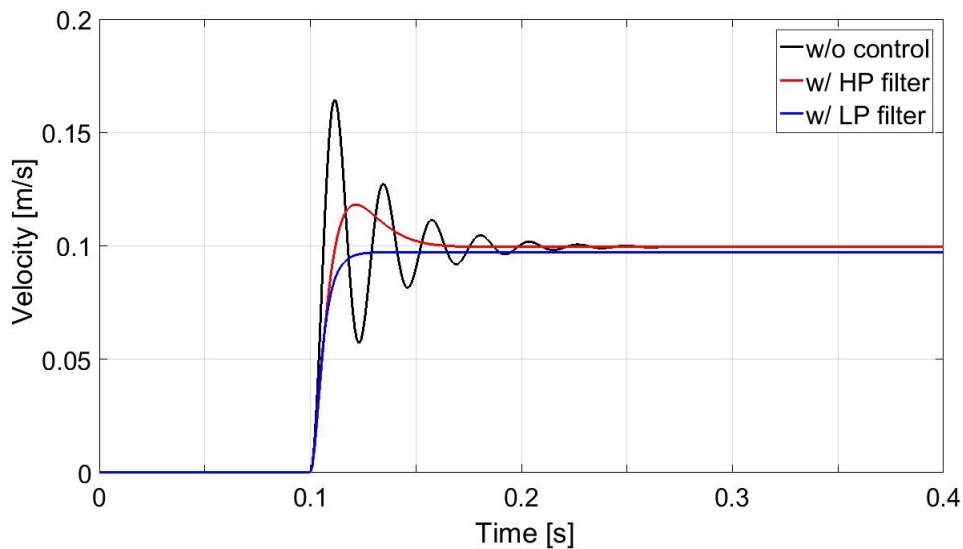
Figure 4.10: Comparison of simulation results with HP filter applied and not

The damping ratio is increased with respect to the original system, therefore, in both piston velocity and pressure inside the actuator chambers, the oscillations are reduced.

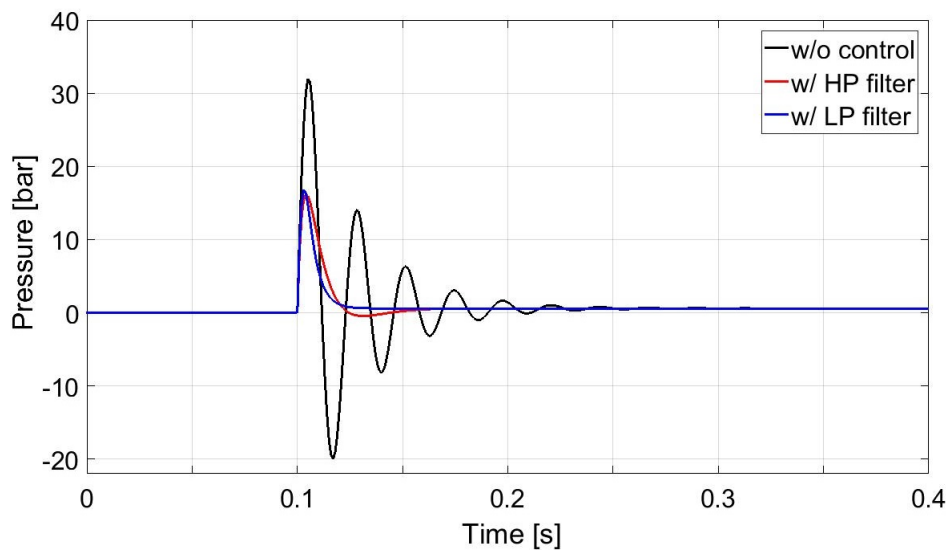
### Comparison

When applying the two filters to the uncompensated system, the purpose is achieved in both conditions. There are only few differences between the two methods, that can lead to choose one or the other, depending on the application.

When commanding a piston velocity of  $0.1 \text{ m/s}$ , the resulting systems behavior are represented in the figures below:



(a) *Piston velocity.*



(b) *Pressure load.*

Figure 4.11: Comparison of simulation results with respect to uncompensated system

As the plots suggest, the damping ratio obtained when the LP filter is implemented is higher. The problem with this method is that, even if the oscillation reduction seems to be better than the one obtainable with the HP filter, there is an error in the steady-state value.

For this reason, when an outer control loop is present, a low pass filter is generally preferable, while, the high pass filter, should be used when there is no control on position or velocity and a reduced load stiffness is not acceptable.

The final choice has been the high pass filter for two main reasons:

- pressure load mean value;
- delay in the resulting signal.

The pressure load signal, in the real application, has a mean value different from zero. The solenoids actuating the spools are controlled depending only on whether the input electric signal is positive or negative and on its amplitude. For this reason, the command the controller should send to the directional valve, instead, has to float around zero. When applying a LP filter, the average value is maintained, while, using an HP filter, the steady state component is removed in the outcome.

Besides, when the oscillatory behavior of the pressure is filtered by a LP filter the resulting signal is delayed with respect to the original one. On the other side, the HP filtered command is closer to the timing of the initial shape.

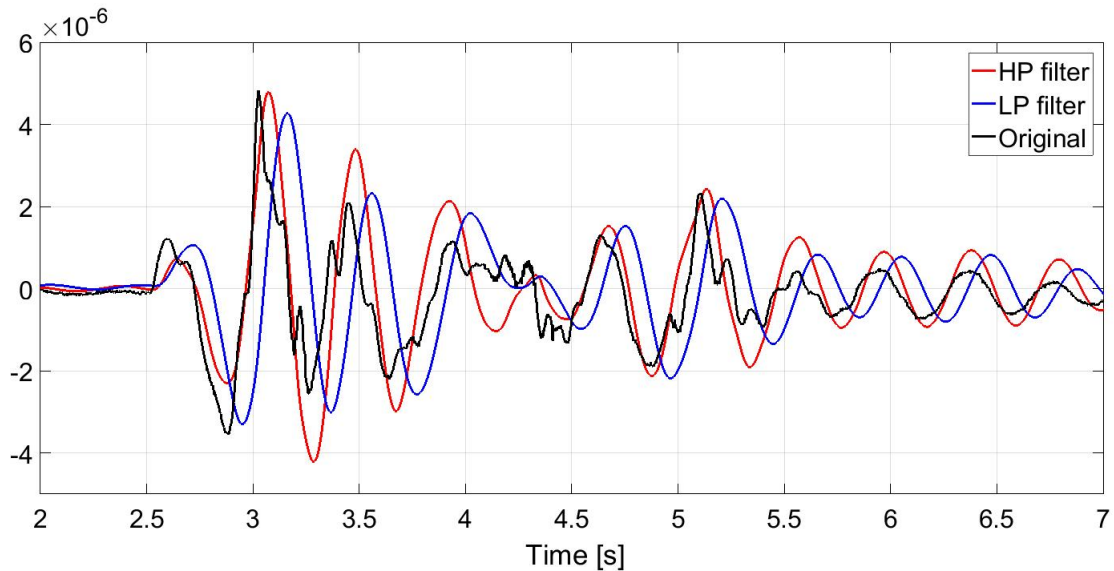


Figure 4.12: Filtered signals delay

In the figure above, a pressure load sample signal, black line, has been filtered through high pass, red line, and low pass filter, blue line. The present delay could cause a very negative result in the control implementation. In fact, since the pressure load vibrates at a relatively high range of frequencies, even a small lateness could affect the correct opening of the valve spools.

## 4.4 Simulation results

Now that the filter has been defined, and its parameters calculated, the controller can be applied to the complete machine model. As for the validation cases, the simulation results will be referred to the two test cases of the wheel loader driven over a speed-bump at different vehicle velocities.

### 4.4.1 Case 1

The simulation results for the first case are the following:

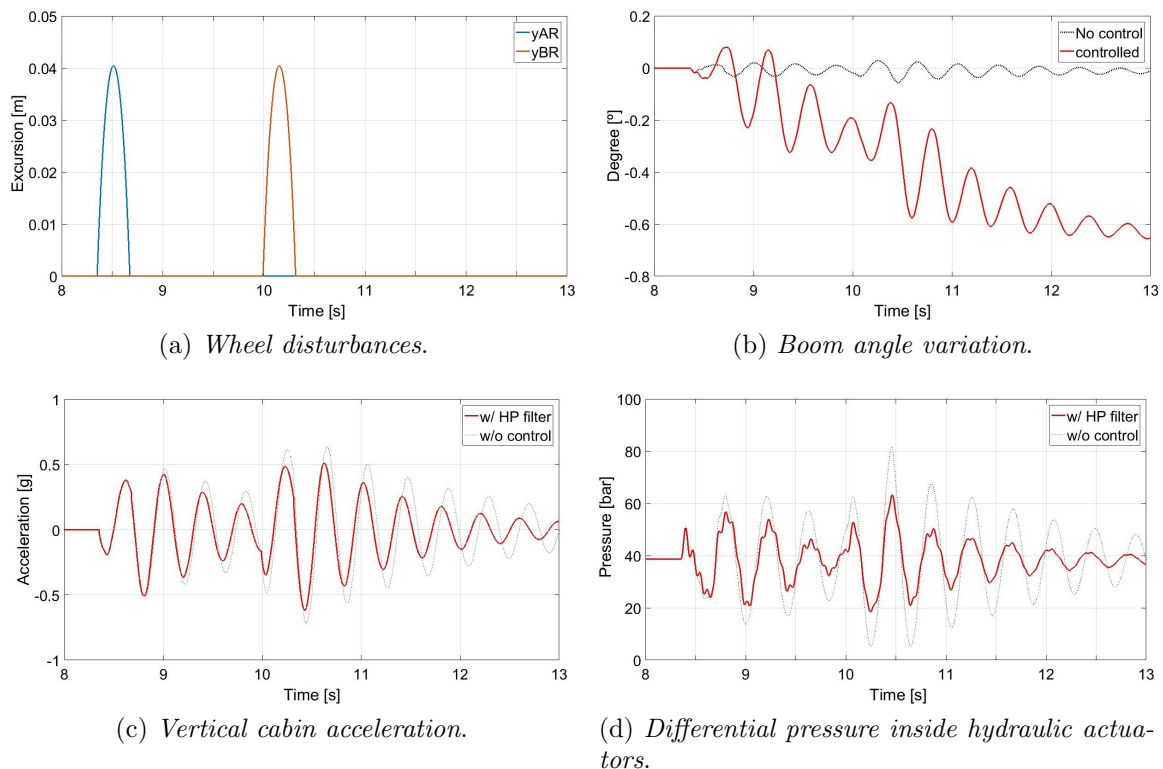


Figure 4.13: First test case control simulation results

There is a good vertical cabin acceleration oscillation reduction, around 27%, and a very evident improvement in the pressure load of the lift actuators, 50%.

In the figure, it's also clear that, with the control implemented, the boom is moving accordingly with the oscillations. Due to the asymmetry of the cylinders, and thus to the area ratio, if not compensated by an adaption of the filter parameters, the arm has the tendency to be lowered.

## 4.4.2 Case 2

The simulation plots for the second case are:

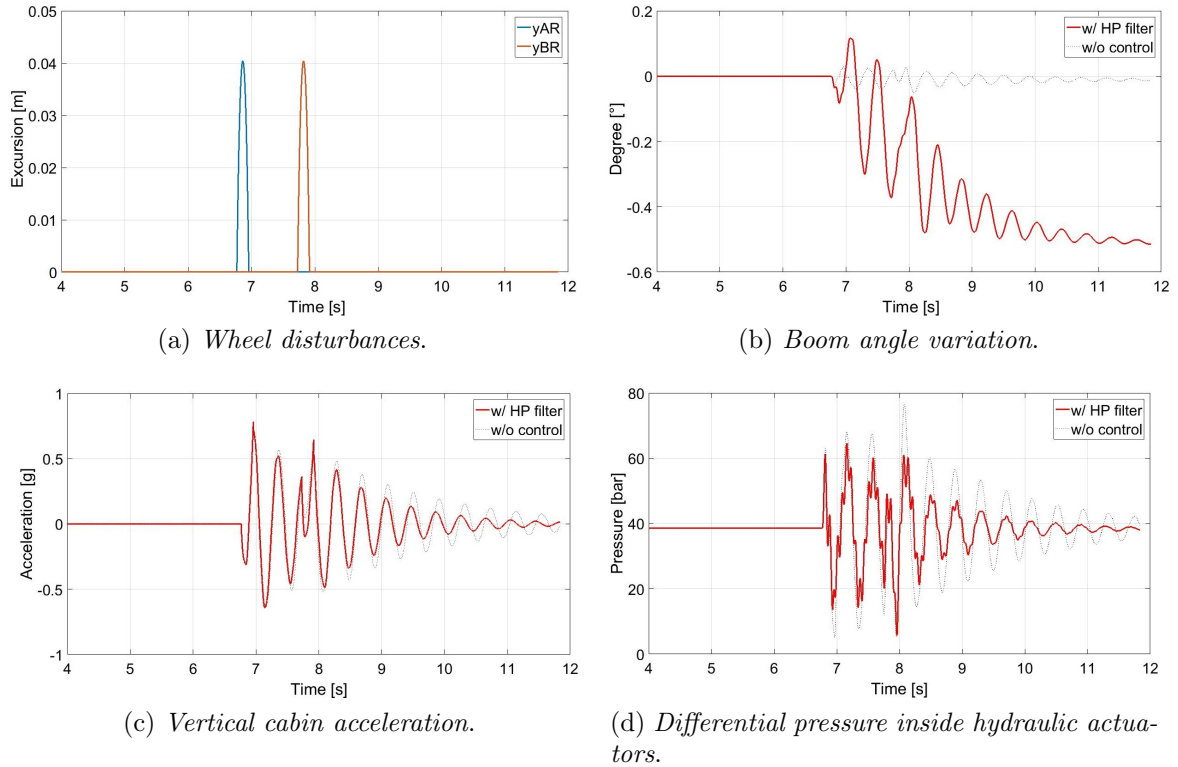


Figure 4.14: Second test case control simulation results

As for the first case, the result is a good oscillations abatement for both cabin acceleration and pressure load, 25% and 45% respectively. Because of the higher vehicle velocity the vertical oscillations are slightly less reduced and there is an higher frequency component in the pressure, causing a not perfectly smooth boom motion.

# Chapter 5

## Experimental results

In this chapter, the first experimental results will be presented. After that, an additional control loop logic, in order to obtain an optimal result, will be shown. Eventually, when the complete controller has been implemented, the tests achievements will be pointed out.

### 5.1 From model to real vehicle

Since the simulation results were promising, I decided to proceed with the experimental implementation on the reference wheel loader. In order to do it, the controller logic has been coded on *LabVIEW*. Through National Instruments devices and wirings, a laptop, provided by the software, has been connected to the pilot stages of the proportional directional valve that manages the flow to the lift actuators cylinders.

The strategy has been proved on the same test cases the simulated model was. The input command, headed to the piloting solenoids, has a range of  $\pm 10$  Volts, where the maximum positive value means complete opening of the spool to obtain the fastest lowering movement, while a negative signal represents a command to raise the boom.

Starting from the first test case, in which the wheel loader hits a speed bump at a low speed, after some parameter tuning to adjust the code to the real system, the first results came up:

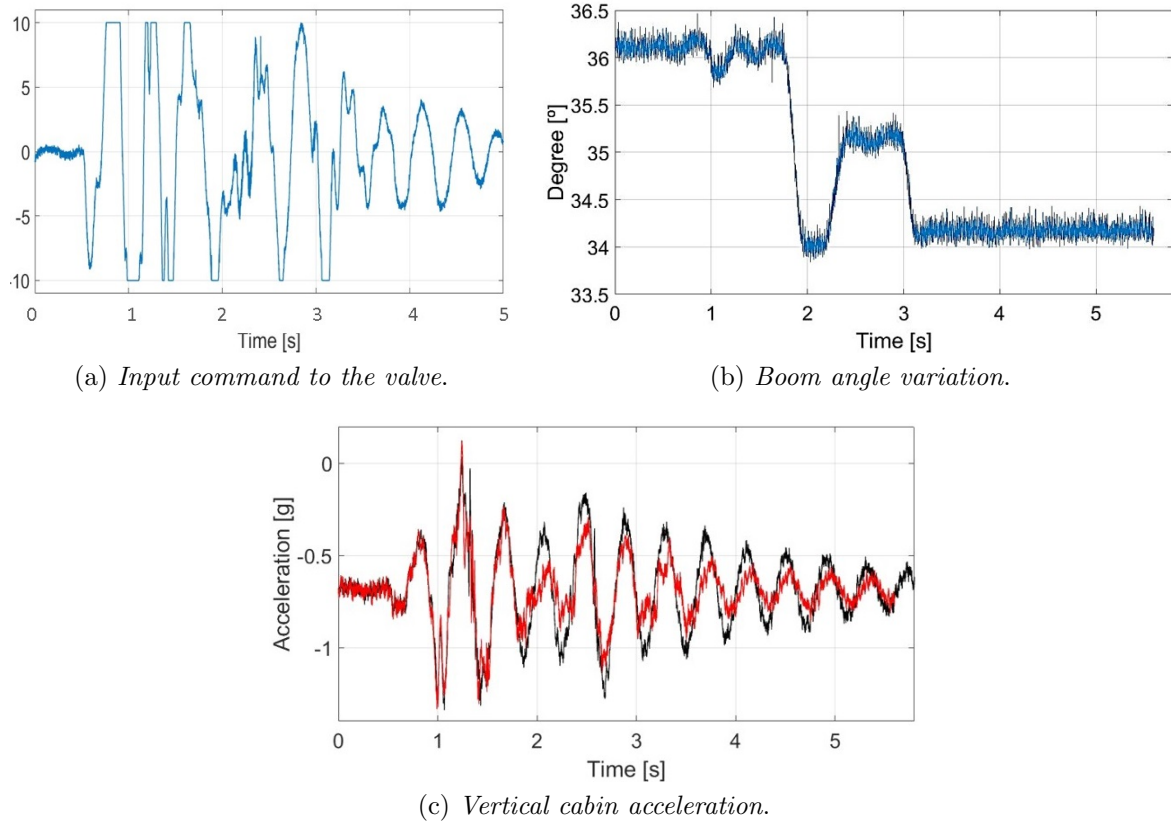


Figure 5.1: First test case control experimental results

From the figures above, it is noticeable a movement of the boom with, as previously mentioned, a tendency towards the bottom. But the arm is not moving accordingly with the command input given by the controller. In fact, the motion is not appreciable until a certain point. Other than on the angle, it particularly affects the oscillations reduction on the cabin. This episode is happening because of the high frequency of the pressure, and thus of the command. The supply is probably not able to follow the dynamics of the input signal in the first moments but, as soon as the frequency slows down, the boom starts moving and the control properly working.

Even if the result is not optimal, a good 30% of oscillations reduction on the vertical cabin acceleration has been obtained.

## 5.2 Position control

Because of the implement angle propensity and due to the too high dynamics of the control signal, I decided to introduce two adjusting gains: one for lowering and the other for raising the boom.

Since a command to move down the arm has an higher responsiveness on the actual movement, the gains have been set so that the lowering actuation had more relevance. In this way, the input signal does not float anymore on the full scale, passing from the bottom command to the top one in few instants, preventing the supply to correctly follow the control action.

When introducing this method, an angle control loop has to be added, otherwise the boom would be lowered even more than before. To do so, I decided to introduce a PD (Proportional-Derivative) block on the feedback loop that, after a set-point angle has been defined, has to keep or restore the established boom position.

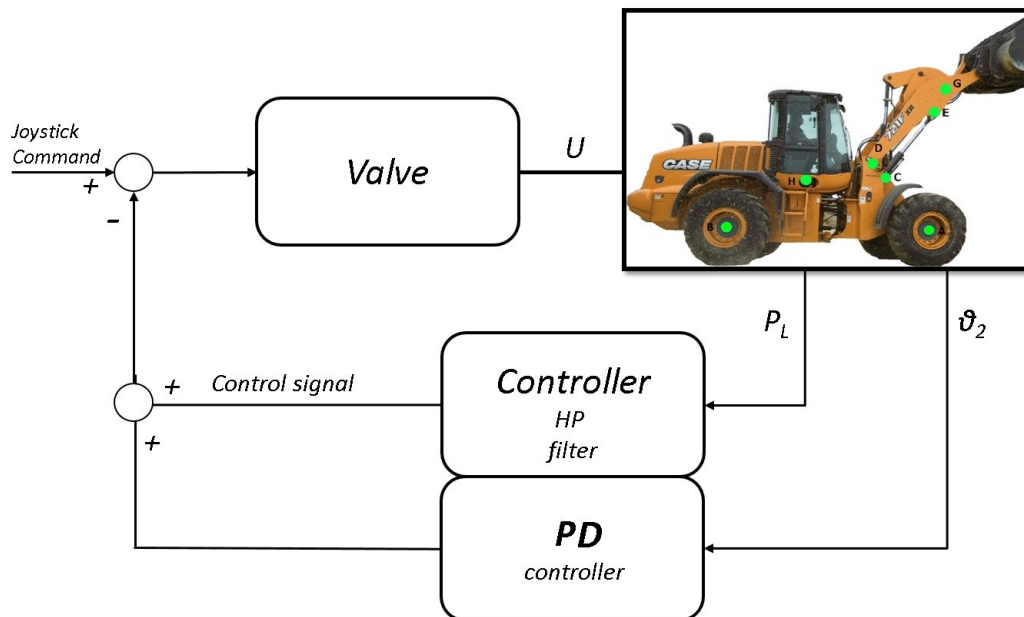


Figure 5.2: Structure schematic with the additional boom angle control loop

The problem with the addition of another control loop is that they could interfere between each other. Since the main controller is the pressure feedback, it should have the priority with respect to the PD.

Some logic has been added to allow it and the schematic below represents the passages the controller does in order to maintain optimal performances on oscillations reduction:

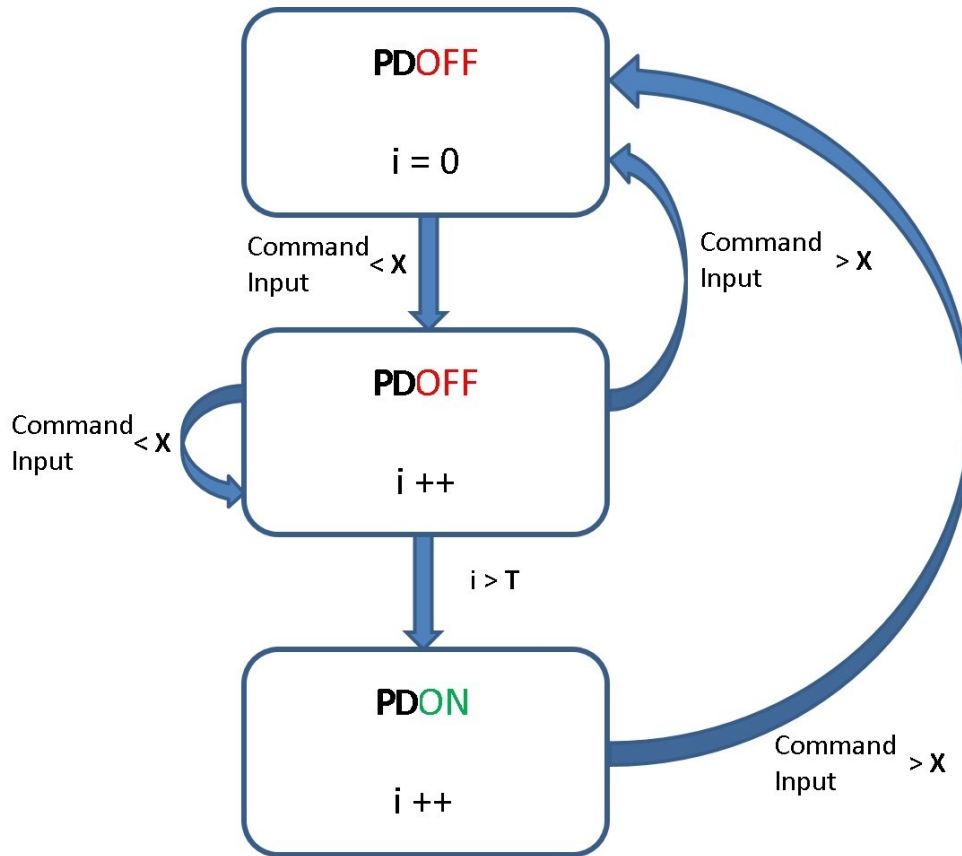


Figure 5.3: State flow for the PD control logic

In the figure above,  $i$  is a parameter that counts steps. Each step corresponds to a certain amount of time, dependent on the *LabVIEW* sampling frequency.  $T$  is a fixed period, or defined number of steps.  $X$  represents a threshold value of the command input.

$i$  increases with the time flowing.  $X$ , being related to the command input amplitude, is also linked to the pressure behavior. In fact, when a big peak is observed in the pressure signal, the controller will send a strong command.

For this reason, starting from the first state, as long as the command input is high, and therefore the oscillations are significant, the PD will stay off. While the oscillations are contained,  $i$  keeps counting and, if the command is still below the selected threshold  $X$ , when the counter goes beyond the period  $T$ , the boom position controller is switched on. But, the instant the input overpasses the set-point, the PD is reset and the cycle starts again.

An example of the applied PD is shown in the figure below:

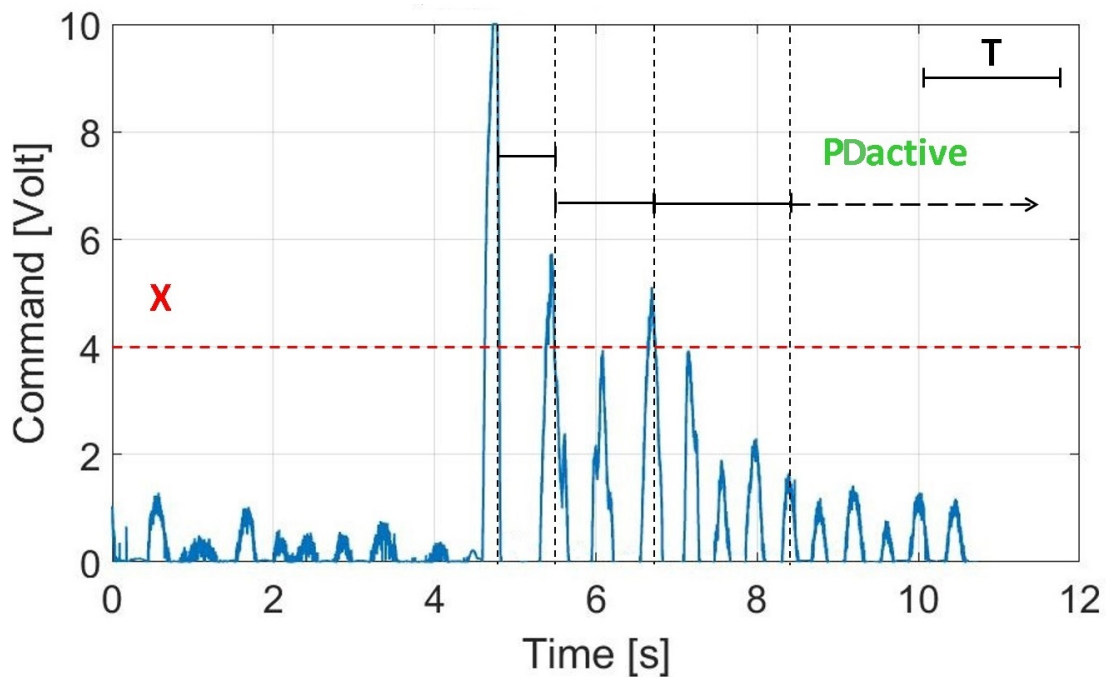


Figure 5.4: PD logic applied, positive input command only

Before any peak is detected the PD is active but, when the wheel loader hit the speed bump, the first one resets the PD state. After that, the  $i$  starts counting, until the next big oscillation overpass the threshold on the command input. When, finally, the counter reaches the value  $T$ , the PD become active.

It must be noted that, both values  $X$  and  $T$  can be selected by the user so that, depending on them, the position control can differently influence the overall controller action.

## 5.3 Complete controller

Once the PD logic has been implemented and the controller structure completed, the following step has been to test it on the speed bump case. It must be noted that, in every figure below, the red curves represent the behavior of the system with controller applied, while the black ones are related to the vehicle without controls

### 5.3.1 Case 1

Considering the scenario in which the vehicle is driven over a hump, at the maximum speed in the first gear, the collected results can be characterized by the figures below:

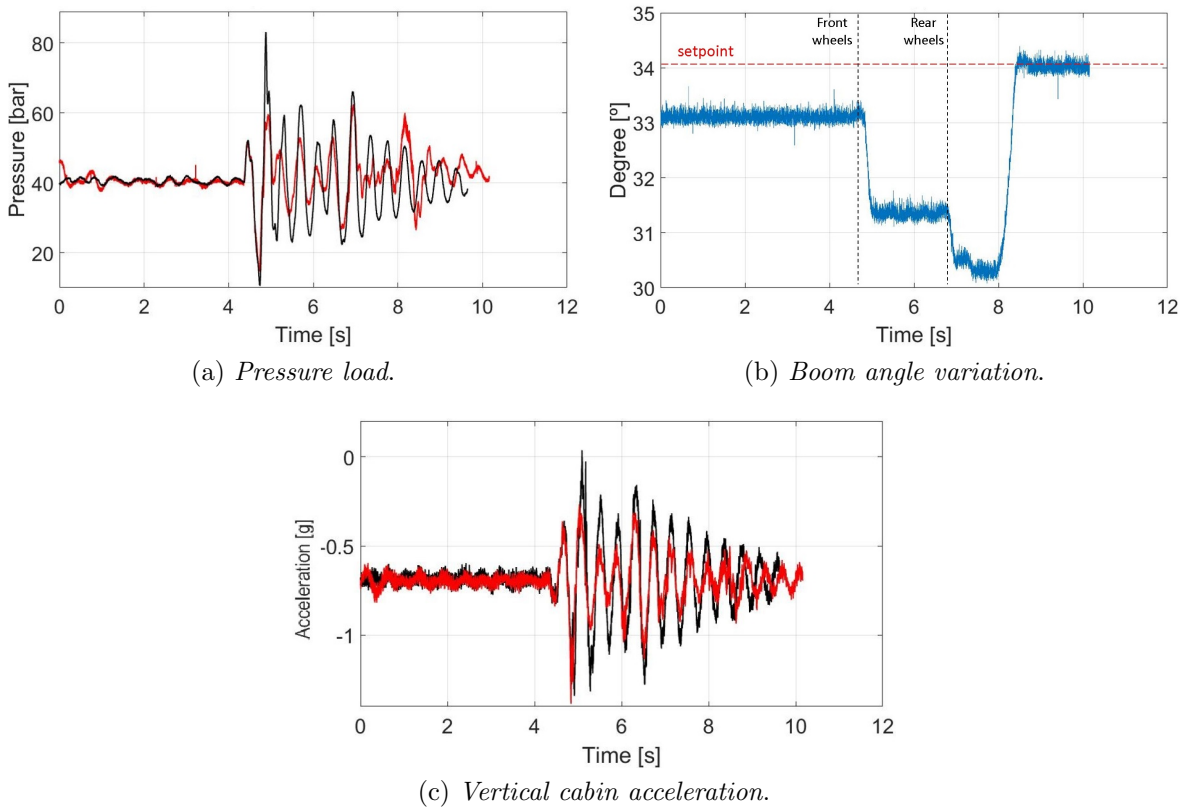


Figure 5.5: Case 1: experimental results long period  $T$

In this example, a relatively long period  $T$  has been chosen.

For this reason, the boom is lowered when the bump is being hit, once due to the front wheels and once due to the rear. After that, the boom established position is restored. The improvement is around 40 % for the vertical cabin acceleration and the driver feelings are much better.

Even though the results are appreciable, with a prolonged chosen period, the improvement is reliable only if the distance between consecutive bumps allows the angle to be brought back to the original position. In fact, if the machine hit two consecutive humps, that are too close between each other, it could happen that the lowering action is too strong.

In order to solve this problem, a shorter period  $T$  could be chosen, so that the outcome would be as the following:

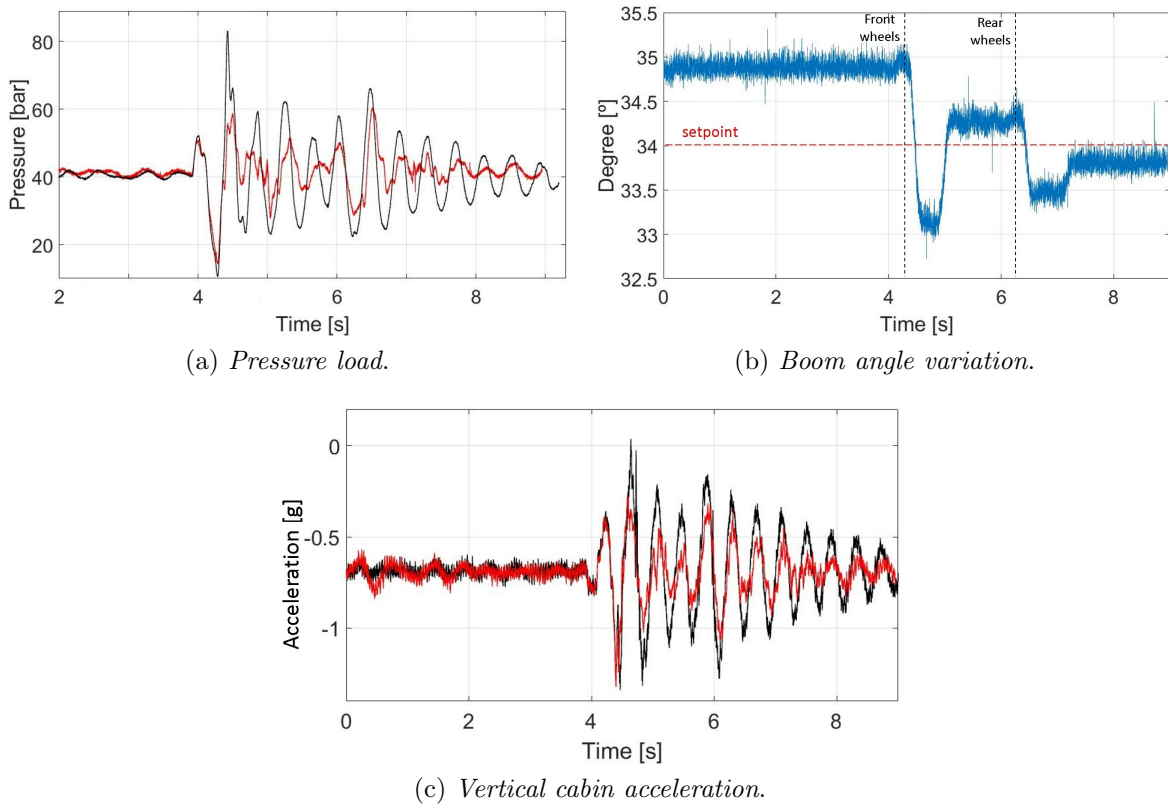


Figure 5.6: Case 1: experimental results short period  $T$

In this case, the improvement is maintained, around 40 %, but the set-point value for the angle is restored in less time. In this way, the vehicle is allowed to pass over multiple bumps, always keeping the boom position around the previously established point.

### 5.3.2 Case 2

When the vehicle passes over a speed bump, at a higher velocity, the behavior is slightly different. Selecting a short period  $T$  for the PD logic, the results are the following:

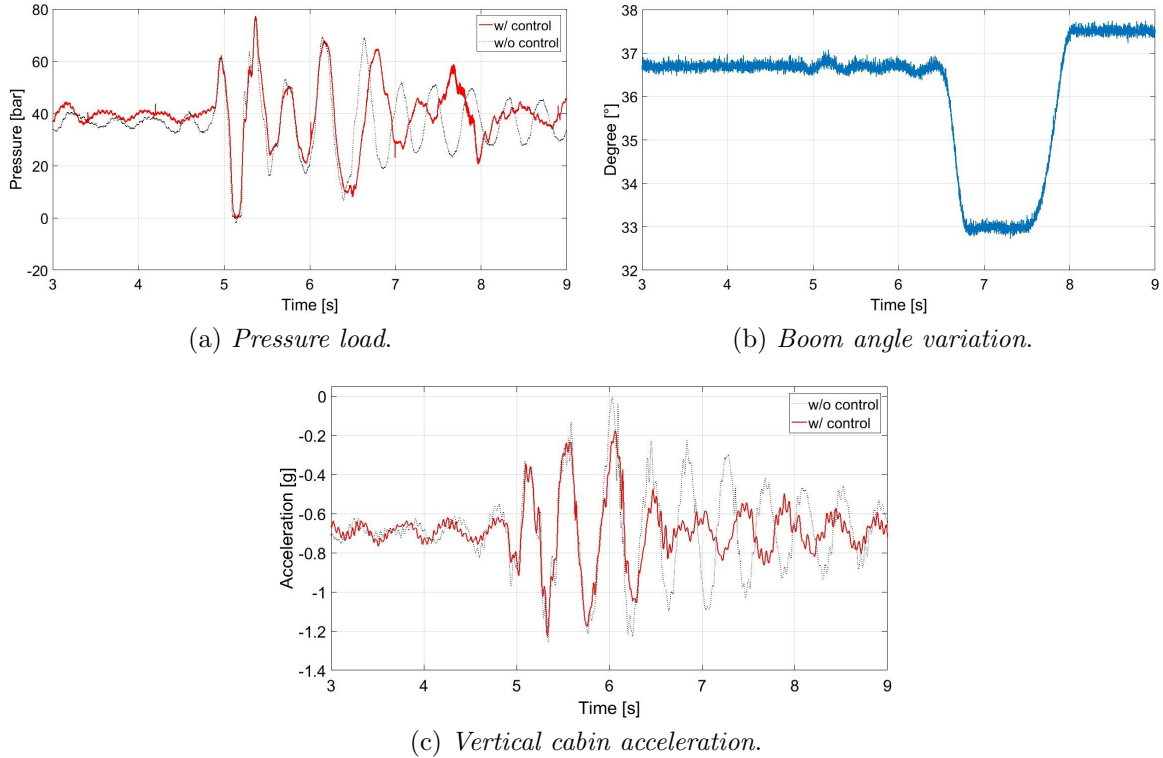


Figure 5.7: Case 2: experimental results short period  $T$

Driving the wheel loader over a speed bump, with an high speed, produces good improvements anyways. The vertical cabin acceleration has an appreciable oscillations reduction as soon as the hump is passed. For what concern the pressure load, the result is not really noticeable since, after the disturbance, the controller sends a strong input in order to quickly restore the boom angle. Because of that, the pressure inside the actuator chambers is strained.

Even if some oscillation is still present on the pressure parameter, during the raising action, the cabin vertical acceleration, and therefore the driver comfort, is not affected by its variation.

# Chapter 6

## Conclusions

As presented in the introductory chapter, off road vehicles with lack of suspensions mounted on the wheels, like a wheel loader, are strained by road oscillations in many different negative ways. An hydro-mechanical solution is already present in the system, called *Passive Ride Control (PRC)*. This method, even if successful in reducing cabin oscillations, is expansive and with a limited range of working effectiveness.

With the objective of achieving an improvement on the machine characteristics, a sample *Active Ride Control (ARC)* has been designed: starting from the achievement of a mathematical model of the vehicle that, once validated with respect to the experimental data, recorded on the field, could provide a way to deduce a proper control structure and a reliable method to test the solution, before implementing it on the real machine.

A control structure has been obtained, simulated and, after that, applied to the vehicle. In order to gain the best result from the current system, another control loop has been added. With the last modification, the control strategy has been completed and, testing it, promising improvements have been collected.

Even if, with the introduction of an active ride control method, the oscillations have been strongly reduced, the passive solution still has better results. For this reason, because of the benefits the system would gain, if the ARC was able to bound the disturbances at least as good as the already present strategy, there are a lot of other steps to make for obtaining an optimal outcome.

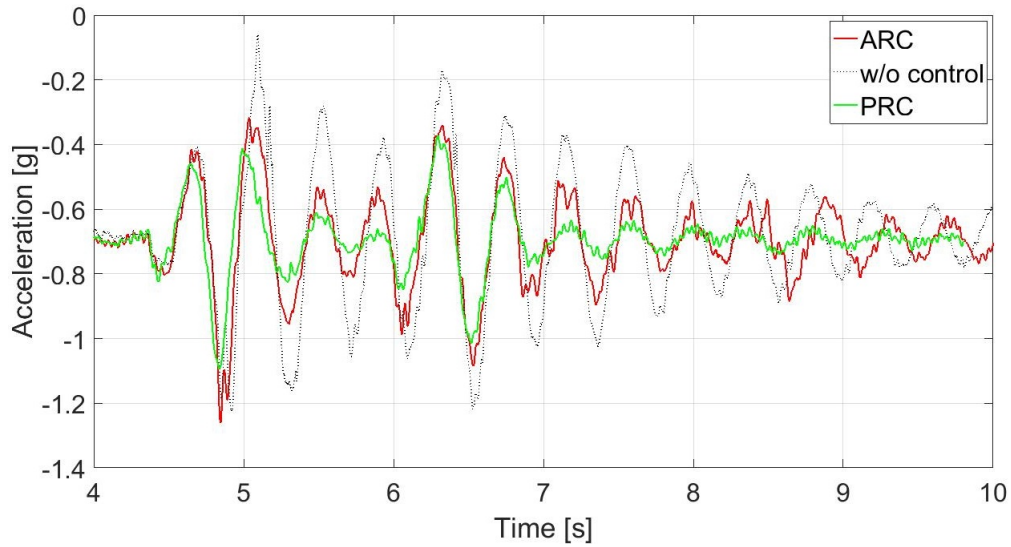


Figure 6.1: Comparison between no control, ARC and PRC

In order to prove the control method potentiality, the wheel loader has also been ridden on a driveway, with random road disturbances. Without operative controls, the vehicle was really unstable. The oscillations were high enough to compromise the machine handling and thus the driver safety. Implementing the studied ARC, the major oscillation peaks have been bounded and, even if the boom had a wide range of angle motion, the overall result has been satisfying and promising.

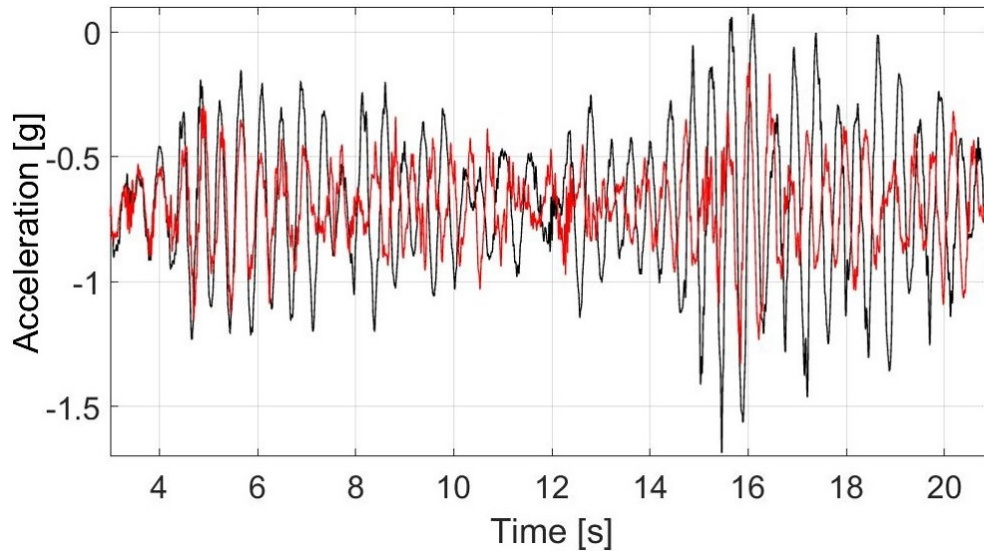


Figure 6.2: Driveway test, vertical cabin acceleration

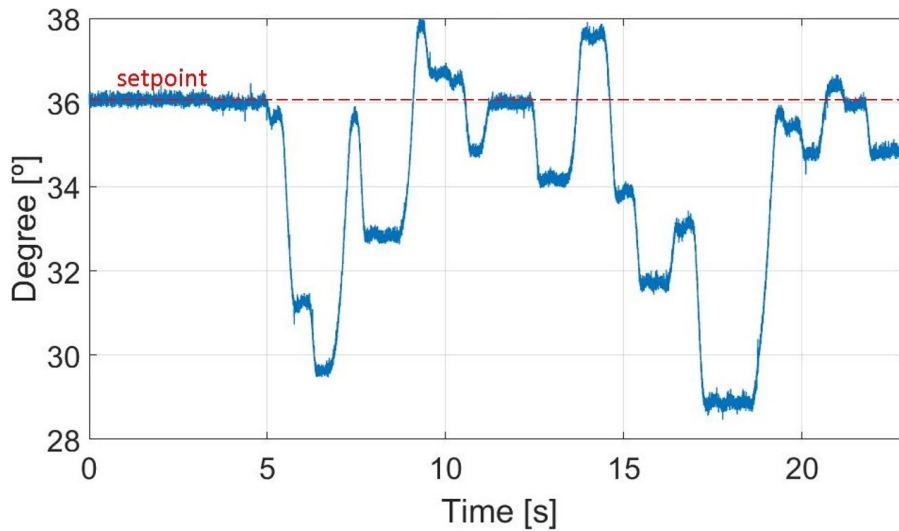


Figure 6.3: Driveway test, boom angle

The gained handling and comfort allow the driver to better ride the vehicle.

On the other hand, the boom angle changes more than expected. But, tuning the control parameters, this problem can be solved, even if the oscillations reduction is slightly less performing with respect to the original set up. For this reason, the two variables have to reach a compromise that, depending on the application, can lead to the best outcome.

Anyway, in the future, the controller can still be modified and improved, until an acceptable result is achieved.

# Chapter 7

## Future work

The ultimate project aim would be to overcome PRC drawbacks and obtain better oscillations reduction with respect to the current damping system. With the studied active method, good achievements have been reached and some strategy gap came out.

Looking at the final results, it's clear that there still is some improvement margin. For reaching better performances something has to be modified.

Analyzing the simulated model, when the supply dynamics is introduced, it can be noticed that the resulting signal is delayed and it has difficulties to follow the commanded frequency. This is mainly caused by the low system responsiveness, and therefor by the supply slowness.

In order to verify this statement I increased the natural frequency characterizing the supply transfer function. Needing less time to respond to commands, the system should be faster now.

Since, on the reference vehicle, the pump has a working frequency fast enough to manage the commands, without changing the hydraulic circuitry, the only modifiable piece is the proportional directional valve that manages the flow to the lift cylinders. For this reason, the variation is to be intended on the valve and not on the rest of the supply.

When the modified block has been introduced in the complete vehicle model, the results can be summarized by the following pictures:

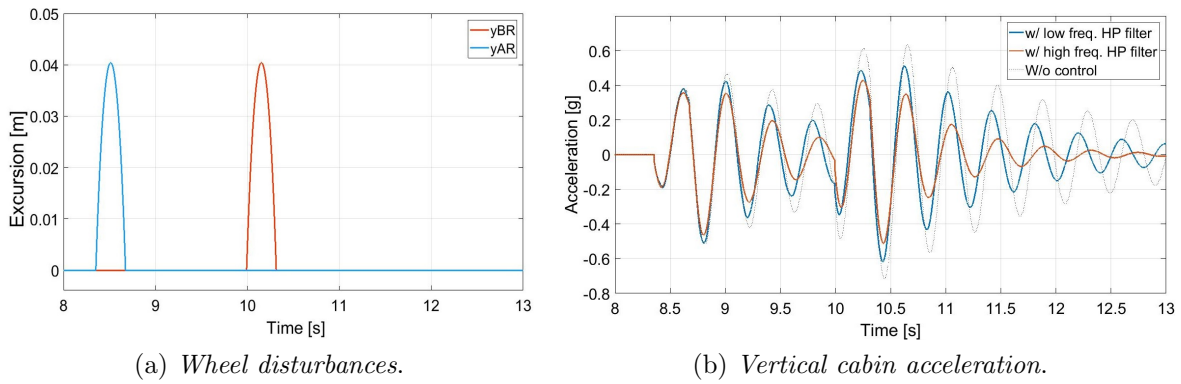


Figure 7.1: First test case control results

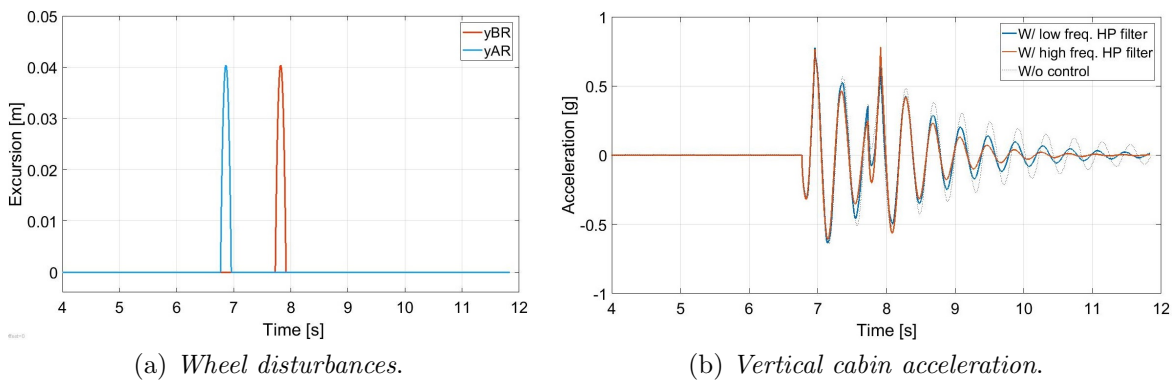


Figure 7.2: Second test case control results

In the first case, when the vehicle speed is lower, the vertical cabin oscillations are reduced of 50 %. Performance becoming really close to the one obtained by the PRC.

In the case on which the speed bump is hit at an higher velocity, the improvement is not as good as for the first test, but still better than the result achieved when the supply dynamics has a lower working frequency.

There still is a lot to investigate on the topic. In fact:

- a faster valve could be purchased and tried on the reference machine;
- a more complex pressure feedback controller could be developed;
- a different feedback variable, for example the vertical cabin acceleration, could be used to build a new controller;
- another way to reduce oscillations, other than moving the boom, could be examined.



# List of Symbols

$m_1$	Mass of the chassis
$m_2$	Mass of the implement
$J_1$	Moment of inertia of the chassis
$J_2$	Moment of inertia of the implement
$F_{*x}$	Horizontal force applied on '*', specific point of the vehicle
$F_{*y}$	Vertical force applied on '*', specific point of the vehicle
$g$	Gravitational force
$r_{12x}$	Distance between 1 and 2 on the horizontal axis
$r_{12y}$	Distance between 1 and 2 on the vertical axis
$\vartheta_{XH}$	Angle between reference point H and 'X'
$\vartheta_{YG}$	Angle between reference point G and 'Y'
$\vartheta_1$	Angle of the chassis
$\vartheta_2$	Angle of the boom
$\dot{\vartheta}_1$	Derivative of the angle of the chassis
$\dot{\vartheta}_2$	Derivative of the angle of the boom
$\ddot{\vartheta}_1$	Double derivative of the angle of the chassis
$\ddot{\vartheta}_2$	Double derivative of the angle of the boom
$x_H$	Horizontal position of center of gravity of the chassis
$x_G$	Horizontal position of center of gravity of the boom
$y_H$	Vertical position of center of gravity of the chassis
$y_G$	Vertical position of center of gravity of the boom
$\dot{x}_H$	Horizontal velocity of center of gravity of the chassis
$\dot{x}_G$	Horizontal velocity of center of gravity of the boom

$\dot{y}_H$	Vertical velocity of center of gravity of the chassis
$\dot{y}_G$	Vertical velocity of center of gravity of the boom
$\ddot{x}_H$	Horizontal acceleration of center of gravity of the chassis
$\ddot{x}_G$	Horizontal acceleration of center of gravity of the boom
$\ddot{y}_H$	Vertical acceleration of center of gravity of the chassis
$\ddot{y}_G$	Vertical acceleration of center of gravity of the boom
$k_{tx}$	Horizontal tire stiffness
$k_{ty}$	Vertical tire stiffness
$c_{tx}$	Horizontal tire damping parameter
$c_{ty}$	Vertical tire damping parameter
$\Delta x_A$	Horizontal displacement of tire A
$\Delta x_B$	Horizontal displacement of tire B
$\Delta y_A$	Vertical displacement of tire A
$\Delta y_B$	Vertical displacement of tire B
$\Delta \dot{x}_A$	Horizontal displacement velocity of tire A
$\Delta \dot{x}_B$	Horizontal displacement velocity of tire B
$\Delta \dot{y}_A$	Vertical displacement velocity of tire A
$\Delta \dot{y}_B$	Vertical displacement velocity of tire B
$x_{AR}$	Horizontal road disturbance on tire A
$x_{BR}$	Horizontal road disturbance on tire B
$y_{AR}$	Vertical road disturbance on tire A
$y_{BR}$	Vertical road disturbance on tire B
$\dot{x}_{AR}$	Derivative of horizontal road disturbance on tire A
$\dot{x}_{BR}$	Derivative of horizontal road disturbance on tire B
$\dot{y}_{AR}$	Derivative of vertical road disturbance on tire A
$\dot{y}_{BR}$	Derivative of vertical road disturbance on tire B
$F_{cyl}$	External force applied to the cylinder
$\gamma$	Angle between lift actuator and horizontal fixed axis

$x_{\text{cyl}}$	Current piston position
$\dot{x}_{\text{cyl}}$	Current piston velocity
$x_{\text{cyl}}^0$	Initial piston position
$l_{\text{cyl}}$	Current actuator length
$l_{\text{cyl}}^0$	Initial actuator length
$V_A$	Volume on A side
$V_B$	Volume on B side
$V_A^0$	Initial volume on A side
$V_B^0$	Initial volume on B side
$A_A$	Area on A side
$A_B$	Area on B side
$m_p$	Piston mass
$A_A$	Area of A flat piston side
$A_B$	Area of B rod side
$p_A$	Pressure inside A flat piston chamber
$p_B$	Pressure inside B rod chamber
$f_V$	Viscous friction coefficient
$f_C$	Columbus friction coefficient
$B$	Bulk modulus
$p_P$	Pump pressure
$p_{LS}$	Load sensing pressure
$A_P$	Area of pump side
$A_{LS}$	Area of LS side
$F_s$	Spring force
$K$	Gain
$\omega_n$	natural frequency
$\zeta$	damping coefficient
$s$	Laplace variable

$\alpha$	Area ratio
$Q_A$	Flow to or from piston chamber
$Q_B$	Flow to or from rod chamber
$P_L$	Differential pressure inside lift actuators
Kf	Filter gain
$\tau$	Filter time constant
LP	Low-pass
HP	High-pass
PD	Proportional derivative
i	Counter
T	Period
X	Set point value for command input
ARC	Active ride control
PRC	Passive ride control

# Bibliography

- [1] R. Bianchi, A. Alexander, and A. Vacca (2016), *Active vibration damping for construction machines based on frequency identification*.
- [2] A. Alexander, A. Vacca, and D. Cristofori (2016), *Active vibration damping in hydraulic construction machinery*.
- [3] Rahmfeld Ivantysynova Eggers (2004), *Active vibration damping for off-road vehicles using valveless linear actuators*.
- [4] Eggers Rahmfeld Ivantysynova (2005), *An energetic comparison between valveless and valve controlled active vibration damping for off-road vehicles*.
- [5] Williamson Ivantysynova (2009), *Active vibration damping for an off-road vehicle with displacement controlled actuators*.
- [6] Henrik C. Pedersen and Torben O. Andersen (2017), *Pressure Feedback in Fluid Power Systems - Active Damping Explained and Exemplified*.
- [7] Cristofori, Davide (2013), *Advanced control strategies for mobile hydraulic applications*.
- [8] DeBoer (2001), *Velocity control of hydraulic cylinders with only pressure feedback*.
- [9] Tommy Ikonen (2006), *Bucket and vehicle oscillation damping for a Wheel Loader*.
- [10] Palmer, M.K., et al. (1998), *Ride Control System*, US Patent 5733095.
- [11] Bosch Rexroth , *Bosch RSM2-25 Stabilizing Module*.

